



Tim Gudmand-Høyer

Behaviour of Concrete Slabs Subjected to Transverse Load and Compressive Axial Forces

Volume 5

Behaviour of Concrete Slabs Subjected to Transverse Load and Compressive Axial Forces

Tim Gudmand-Høyer

1 Preface

This report is prepared as a partial fulfilment of the requirements for obtaining the Ph.D. degree at the Technical University of Denmark.

The work has been carried out at the Department of Structural Engineering and Materials, Technical University of Denmark (BYG•DTU), under the supervision of Professor, dr. techn. M. P. Nielsen.

I would like to thank my supervisor for valuable advise, inspiration and many rewarding discussions and criticism to this work.

Thanks are also due to my co-supervisor M. Sc. Ph.D. Bent Steen Andreasen, RAMBØLL, M. Sc. Ph.D.-student Karsten Findsen, BYG•DTU, M. Sc. Ph.D.-student Lars Z. Hansen, BYG•DTU, M. Sc. Ph.D.-student Thomas Hansen, BYG•DTU and M. Sc. Ph.D.-student João Luís Garcia Domingues Dias Costa, BYG•DTU for their engagement and criticism to the present work and my Ph.D.-project in general.

Finally I would like to thank my wife and family for their encouragement and support.

Lyngby, August 2004

Tim Gudmand-Høyer

2 Summary

This paper treats the behaviour of concrete slabs subjected to lateral load and compressive axial force.

The assumptions regarding the material behaviour are described in [14] and this paper demonstrates how to incorporate the stiffnesses found in [14] in the determination of slab behaviour.

The subject is approached from a practical point of view. Thus, the solutions should be fairly simple without being too far from the exact ones.

Generally the behaviour is determined from an estimation of the deflection form and the use of the work equation. This means that the solutions are upper bound solutions and the equilibrium equations are not necessarily fulfilled.

Slabs subjected to transverse load, axial load or a combination, and with different support conditions are treated theoretically. It is demonstrated how to determine the relation between axial force, transverse load and deflection.

The report is limited to compressive axial force only.

One test series has been used to demonstrate the practical use of the method and good agreement has been found.

3 Resume

Denne rapport behandler emnet betonplader påvirket af tryknormalkræfter og tværlast. Antagelser vedrørende materialeopførelse er beskrevet i rapporten Stiffness of concrete slabs, se [14], og nærværende rapport demonstrer hvordan man kan anvende disse stivheder til bestemmelse af pladens opførsel.

Emnet behandles ud fra en praktisk synsvinkel. Det er tilstræbes at beskrive den overordnede opførsel af pladen på en simpel måde uden at være for langt fra eksakte løsninger.

Beregningsmetoden er baseret på et udbøjningsskøn samt anvendelse af energiligningen. Dette betyder at der er tale om en øverværdiløsning og at ligevægtsbetingelserne ikke nødvendigvis er opfyldt.

Plader påvirket med normalkræfter, tværlast eller en kombination af disse er behandlet teoretisk og de fundne resultater er eksemplificeret med forskellige pladetyper og forskellige armeringsplaceringer.

Rapporten behandler kun tryknormalkræfter.

Til verificering af beregningsmetoden er der foretaget en sammenligning mellem teori og eksperimenter for en forsøgsserie. Der blev her fundet god overensstemmelse.

4 Table of contents

| | | |
|-------|---|----|
| 1 | Preface..... | 1 |
| 2 | Summary | 3 |
| 3 | Resume..... | 4 |
| 4 | Table of contents..... | 5 |
| 5 | Notation..... | 7 |
| 6 | Introduction..... | 9 |
| 7 | Theory | 11 |
| 7.1 | GENERAL EQUATIONS | 11 |
| 7.1.1 | Constitutive equations..... | 11 |
| 7.1.2 | Compatibility conditions..... | 16 |
| 7.1.3 | Equilibrium equations..... | 17 |
| 7.1.4 | Boundary conditions | 17 |
| 7.2 | DEFLECTIONS OF SLABS WITH NO AXIAL FORCE | 19 |
| 7.2.1 | Estimation of deflections using Rayleigh's principle | 19 |
| 7.2.2 | Beam example..... | 19 |
| 7.2.3 | Rectangular slab simply supported at all sides | 21 |
| 7.2.4 | Rectangular slab simply supported at three sides and one free edge | 23 |
| 7.2.5 | Rectangular slab fixed at all sides..... | 27 |
| 7.2.6 | Rectangular slab with two adjacent sides fixed and two sides free | 28 |
| 7.2.7 | Rectangular slab with two adjacent sides simply supported and two sides free | 29 |
| 7.2.8 | Exemplification of deflection calculations | 30 |
| 7.3 | STABILITY OF SLABS LOADED WITH AXIAL FORCE | 32 |
| 7.3.1 | Rectangular slab simply supported at all sides | 33 |
| 7.3.2 | Rectangular slab simply supported at three sides and one free edge | 34 |
| 7.3.3 | Rectangular slab fixed at all sides..... | 35 |
| 7.3.4 | Rectangular slab with two adjacent sides fixed and two sides free | 35 |
| 7.3.5 | Rectangular slab with two adjacent sides simply supported and two sides free | 36 |
| 7.3.6 | Exemplification of stability calculations..... | 36 |

| | | |
|-------|--|----|
| 7.4 | DEFLECTIONS OF SLABS WITH AXIAL FORCE..... | 40 |
| 7.4.1 | Rectangular slab simply supported at four sides loaded with an axial force in one direction | 40 |
| 8 | Theory compared with tests..... | 49 |
| 9 | Conclusion | 58 |
| 10 | Literature | 59 |
| 11 | Appendix | 61 |
| 11.1 | DESCRIPTION OF COMPUTER PROGRAM | 61 |

5 Notation

The most commonly used symbols are listed below. Exceptions from the list may appear, but this will then be noted in the text in connection with the actual symbol.

Geometry

| | |
|--------------------|--|
| L | Length of a beam |
| L_x, L_y | Length of a slab in the x - and y - direction, respectively |
| h | Depth of a cross-section |
| h_c | Distance from the bottom face to the centre of the bottom reinforcement |
| h_c' | Distance from the top face to the centre of the top reinforcement |
| h_{cx}, h_{cy} | Distance from the bottom face to the centre of the bottom reinforcement in the x - and y - direction, respectively |
| h_{cx}', h_{cy}' | Distance from the top face to the centre of the top reinforcement in the x - and y - direction, respectively |
| d | Effective depth of the cross-section, meaning the distance from the top the slab to the centre of the reinforcement. |
| A | Area of a cross-section |
| A_c | Area of a concrete cross-section |
| A_s | Area of reinforcement per unit length close to the bottom face |
| A_s' | Area of reinforcement per unit length close to the top face |
| A_{sx}, A_{sy} | Area of reinforcement per unit length close to the bottom face in the x - and y - direction, respectively |
| A_{sx}', A_{sy}' | Area of reinforcement per unit length close to the top face in the x - and y - direction, respectively |
| y_0 | Compression depth |
| x, y, z | Cartesian coordinates |

Physics

| | |
|----------------------------|---|
| σ | Normal stress |
| σ_c | Normal stress in concrete |
| σ_{cx}, σ_{cy} | Normal stress in concrete in the x - and y - direction, respectively. |

| | |
|---|--|
| f_c | Compressive strength of the concrete. |
| ϕ | Reinforcement ratio |
| $n\phi$ | Degree of reinforcement |
| ϕ_x, ϕ_x' | Reinforcement ratio in the x -direction for the lower and upper reinforcement, respectively. |
| ϕ_y, ϕ_y' | Reinforcement ratio in the y -direction for the lower and upper reinforcement, respectively. |
| E | Modulus of elasticity |
| E_s | Modulus of elasticity for the reinforcement |
| E_c | Modulus of elasticity for the concrete |
| n | Ratio between the modulus of elasticity for the reinforcement and the modulus of elasticity for the concrete |
| D_x, D_y | Bending stiffness for the slab in the x and y -direction, respectively |
| D_{xy} | Torsional stiffness for the slab |
| n_x, n_y | Axial load per unit length in the x - and y -direction, respectively. Positive as compression. |
| n_{xy} | Shear load per unit length |
| m_x, m_y | Bending moment per unit length in the x - and y -direction, respectively |
| m_{xy} | Torsional moment per unit length |
| q_x, q_y | Transverse shear load per unit length in the x - and y -direction, respectively |
| $\tilde{m}_n, \tilde{m}_x, \tilde{m}_y$ | Applied bending moment per unit length at the edge in the n -, x - and y -direction, respectively |
| $\tilde{q}_n, \tilde{q}_x, \tilde{q}_y$ | Applied transverse shear load per unit length at the edge in the n -, x - and y -direction, respectively |
| p | Transverse load |
| u | Transverse deflection |
| κ_x, κ_y | Curvature in the x and y -direction, respectively |
| κ_{xy} | Torsional curvature |

6 Introduction

This paper demonstrates how to incorporate the stiffnesses found in [14] in determination of slab behaviour. It is assumed that the reader is familiar with [14] and expressions and definitions from this report is used here without further explanation.

The first section describes the constitutive equations, the compatibility conditions and the boundary conditions used in this investigation.

The next section treats slabs subjected to transverse load only. The method used in this investigation is first described in general and then followed by five determinations of the slab stiffnesses for some of the most common support conditions of rectangular slabs.

Two reinforcement arrangements, one with the reinforcement placed in the centre and one where it is placed close to the faces, are used for exemplifications.

Similar approach is used in the following section that treats slabs subjected to axial force only. The stability loads for the five slab cases mentioned above are determined and the same two reinforcement arrangements are used for exemplification.

The general approach used for a combination of lateral load and axial force is described in the next section. A rectangular slab, simply supported at all sides with axial force in two directions, is used for demonstrating the method. In this section some considerations regarding the importance of the loading history of the slab are made as well.

As a verification of the method, test results from a series with square slabs subjected to axial force in one direction are compared with calculations. Good agreement is found.

In the final section conclusions are made.

7 Theory

7.1 General equations

7.1.1 Constitutive equations

The constitutive equations assumed in this investigation are:

$$\begin{aligned} m_x &= D_x \kappa_x = -D_x \frac{\partial^2 u}{\partial x^2} \\ m_y &= D_y \kappa_y = -D_y \frac{\partial^2 u}{\partial y^2} \\ m_{xy} &= D_{xy} \kappa_{xy} = -D_{xy} \frac{\partial^2 u}{\partial x \partial y} \end{aligned} \quad (7.1.1)$$

The bending stiffness and the torsional stiffness found in [14] are used.

Only a short explanation of the calculations is given here. For a thorough treatment the reader is referred to [14].

In [14] it is shown that the stiffness may be calculated as a function of the degree of cracking. The degree of cracking is the ratio between the cracking moment and the applied moment. The cracking moment is defined as the transition point between the cracked and the uncracked state.

For pure bending the cracking moment may be calculated by:

$$m_{x,crack} = \frac{n_x h \left(\frac{1}{12} + \left(-\frac{1}{2} \frac{h_c}{h} + \left(\frac{h_c}{h} \right)^2 \right) n\phi + \left(\frac{1}{2} - \frac{3}{2} \frac{h_c'}{h} + \left(\frac{h_c'}{h} \right)^2 \right) n\phi' \right)}{\frac{1}{2} + n\phi \frac{h_c}{h} + n\phi' \left(1 - \frac{h_c'}{h} \right)} \quad (7.1.2)$$

where n_x is the axial force per unit length, n is the ratio between the modulus of elasticity for the reinforcement and the modulus of elasticity for the concrete (E_s/E_c), h is the thickness of the slab, h_c is the distance from the bottom face to the lower layer of reinforcement, h_c' is the distance from the top face to the upper layer of reinforcement, ϕ is the reinforcement ratio for the lower reinforcement layer and ϕ' is the reinforcement ratio for the upper reinforcement layer both based on the total section.

In the special case with only one layer of reinforcement placed in the centre of the slab we get:

$$m_{x,crack} = \frac{1}{6} \frac{n_x h}{1 + n\phi} \quad (7.1.3)$$

It was shown that besides the physical properties of the slab the bending stiffness only depends on the $n_x h/m_x$ ratio. The limits for $n_x h/m_x$ corresponding to $y_0=h$ and $y_0=0$ becomes:

$$\frac{n_x h_{(y_0=h)}}{m_x} = \frac{\frac{1}{2} + n\phi \frac{h_c}{h} + n\phi' \left(1 - \frac{h_c'}{h}\right)}{\frac{1}{12} + \left(-\frac{1}{2} \frac{h_c}{h} + \left(\frac{h_c}{h}\right)^2\right) n\phi + \left(\frac{1}{2} - \frac{3}{2} \frac{h_c'}{h} + \left(\frac{h_c'}{h}\right)^2\right) n\phi'} \quad (7.1.4)$$

$$\frac{n_x h_{(y_0=0)}}{m_x} = \frac{-2 \left(\phi \left(1 - \frac{h_c}{h}\right) + \phi' \frac{h_c'}{h} \right)}{\phi \left(1 - 3 \frac{h_c}{h} + 2 \left(\frac{h_c}{h}\right)^2\right) + \phi' \left(-\frac{h_c'}{h} + 2 \left(\frac{h_c'}{h}\right)^2\right)} \quad (7.1.5)$$

Notice that n_x and n_y are positive as compression.

If the $n_x h/m_x$ ratio is higher than the limit for $y_0=h$ the stiffness of the slab will be the uncracked stiffness given by:

$$\frac{D_{x(y_0=h)}}{h^3 E_c} = \frac{1}{12} + \left(\left(\frac{h_c}{h}\right)^2 - \frac{1}{2} \frac{h_c}{h} \right) n\phi + \left(\frac{1}{2} - \frac{3}{2} \frac{h_c'}{h} + \left(\frac{h_c'}{h}\right)^2 \right) n\phi' \quad (7.1.6)$$

If the $n_x h/m_x$ ratio is lower than the limit for $y_0=0$ the stiffness equals the stiffness of the reinforcement only given by:

$$\frac{D_{x(y_0=0)}}{h^3 E_c} = \left(\frac{1}{2} + \left(\frac{h_c}{h}\right)^2 - \frac{3}{2} \frac{h_c}{h} \right) n\phi + \left(\left(\frac{h_c'}{h}\right)^2 - \frac{1}{2} \frac{h_c'}{h} \right) n\phi' \quad (7.1.7)$$

In Figure 7.1 and Figure 7.2 the stiffnesses as a function of the degree of cracking are shown for two types of slabs. The first type is valid for slabs with reinforcement in the centre and the second type is valid for the reinforcement placed symmetrically about the centre, close to the faces. These are the two types generally used in this investigation.

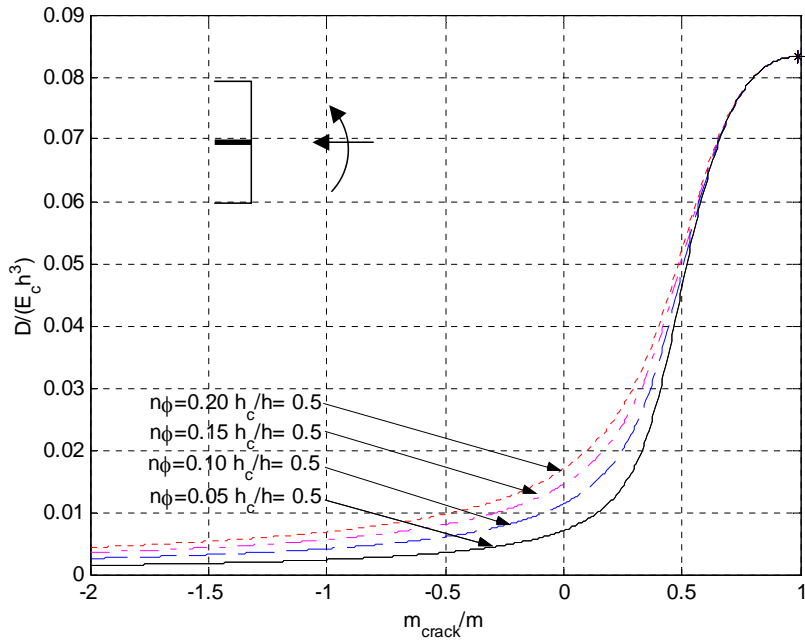


Figure 7.1 Bending stiffness as a function of the cracking moment over moment ratio. $h_c = 1/2h$. One layer of reinforcement.

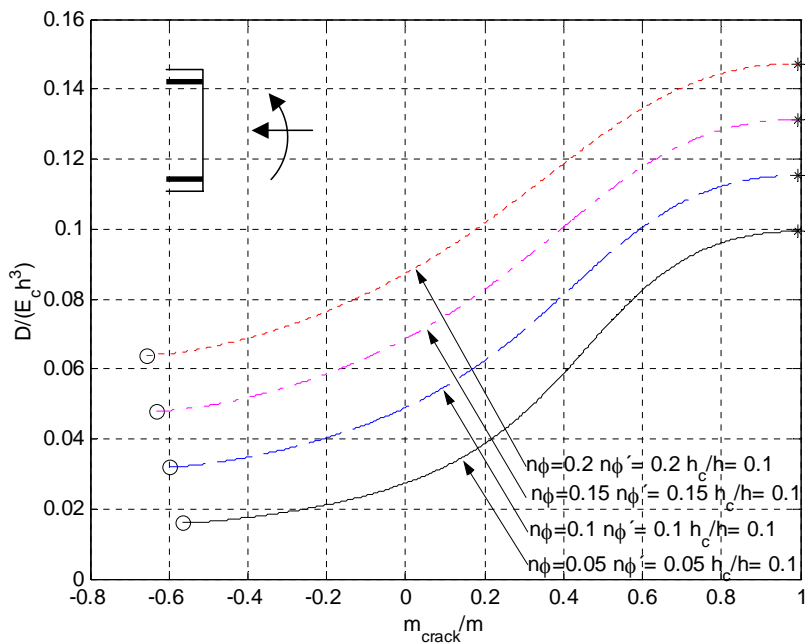


Figure 7.2 Bending stiffness as a function of the cracking moment over moment ratio. $h_c = h_c' = 0.1h$. Two layers of reinforcement.

In [14] it was found that the torsional stiffness dependency on the degree of cracking is the same as the bending stiffness dependency on the degree of cracking for a slab with the reinforcement placed in the centre. This means that the torsional stiffness is simply found by “moving” the reinforcement to the centre of the slab and then calculate the bending stiffness. This procedure is illustrated in Figure 7.3.

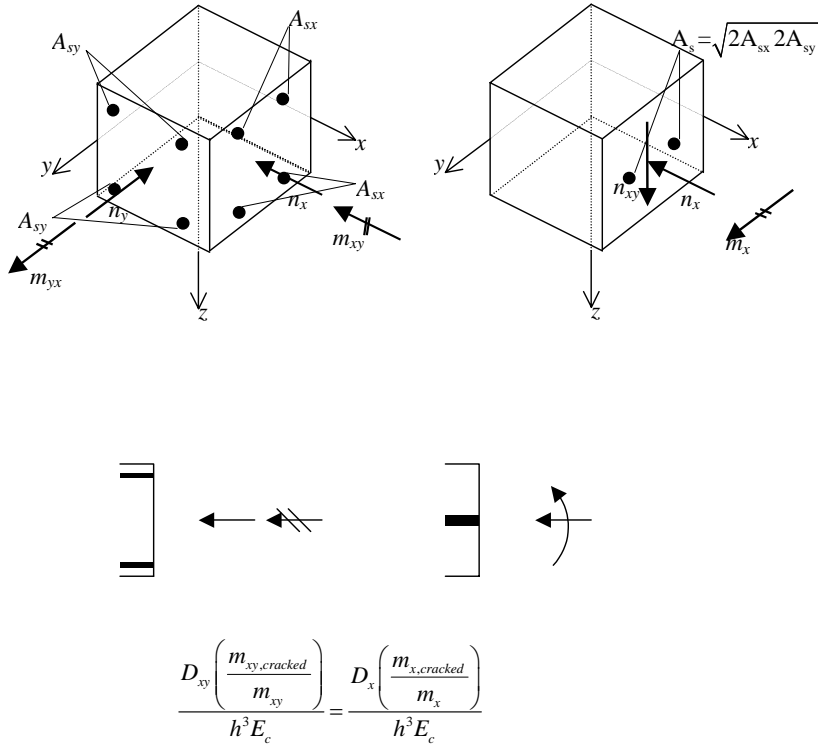


Figure 7.3. The relation between torsional- and bending stiffness for an isotropic slab.

This means that diagrams for bending stiffnesses may be used if the degree of cracking for torsion is replaced by the degree of cracking for bending. The degree of cracking for torsion may be calculated from the cracking moment given by:

$$m_{xy,crack} = \text{sign}(n_y) \frac{h \sqrt{n_y (1 + 2\phi_y n) (1 + 2\phi_x n) n_x}}{6(1 + 2\phi_y n + 2\phi_x n + 4\phi_x n \phi_y n)} \quad (7.1.8)$$

It should be noted that this ratio may only be used for axial forces of the same sign which is assumed throughout the report if nothing else is stated.

Furthermore, the cracking moment does not have any meaning if one of the axial forces is zero. In this case the cracking moment would always be zero meaning that the torsional stiffness is independent of the axial force, which is of course not correct. However, this problem will be ignored in this report and we shall assume that the cracking moment concept may also be used if one of the axial forces is zero. This means that the torsional stiffness for a slab loaded by axial force in one direction will be the same as for a slab without any axial load.

It should be noted that the influence of bending moments on the torsional stiffness, and the influence of the torsional moment on the bending stiffnesses have not been investigated neither in [14] nor here. Thus, the stiffnesses are assumed to be independent of each other.

7.1.1.1 Exemplification of the stiffnesses

As an example we consider a slab section with the reinforcement placed close to the face. This is named a case 2 arrangement. For a section without any axial force the degree of cracking is zero and the stiffnesses therefore are only depending on the degree of reinforcement. Assuming a degree of isotropic reinforcement of $n\phi=n\phi'=0.1$ we find, using Figure 7.2, that the bending stiffness is:

$$\frac{D_x}{E_c h^3} = \frac{D_y}{E_c h^3} \approx 0.05 \quad (7.1.9)$$

The torsional stiffness is found from Figure 7.1 using a fictitious degree of reinforcement of $n\phi=0.2$ which takes into account both layers of reinforcement. Thus the torsional stiffness becomes:

$$\frac{D_{xy}}{E_c h^3} \approx 0.017 \quad (7.1.10)$$

If we consider a slab section with only one layer of isotropic reinforcement placed in the centre, named a case 1 arrangement, having a degree of reinforcement of $n\phi=0.2$, we find that in this case the stiffness becomes:

$$\frac{D_x}{E_c h^3} = \frac{D_y}{E_c h^3} = \frac{D_{xy}}{E_c h^3} \approx 0.017 \quad (7.1.11)$$

As seen the position of the reinforcement is decisive for the ratio of the bending and torsional stiffness. If the reinforcement is placed in the centre, the bending and torsional stiffnesses are the same and if the reinforcement is placed close to the faces the torsional stiffness is only about 1/3 of the bending stiffness. This conclusion is only valid for cases without axial force. If axial force is applied, the ratio between the stiffnesses changes as a function of the axial force.

If we consider the uncracked state the stiffnesses in case 1 (reinforcement in the centre $n\phi=0.2$) becomes:

$$\frac{D_x}{E_c h^3} = \frac{D_y}{E_c h^3} = \frac{D_{xy}}{E_c h^3} \approx 0.083 \quad (7.1.12)$$

In case 2 (isotropic reinforcement close to the faces, $n\phi=n\phi'=0.1$, $hc/h=0.1$) we have:

$$\begin{aligned} \frac{D_{xy}}{E_c h^3} &\approx 0.083 \\ \frac{D_x}{E_c h^3} &= \frac{D_y}{E_c h^3} \approx 0.115 \\ D_x &= D_y = 1.4 D_{xy} \end{aligned} \quad (7.1.13)$$

If the bending stiffness in the x -direction is calculated for uncracked concrete and if the bending stiffness in the y -direction as well as the torsional stiffness are calculated for cracked concrete, we get:

In case 1:

$$\begin{aligned} \frac{D_x}{E_c h^3} &\approx 0.083 \\ \frac{D_y}{E_c h^3} &= \frac{D_{xy}}{E_c h^3} \approx 0.017 \\ D_x &= 4.9 D_y = 4.9 D_{xy} \end{aligned} \quad (7.1.14)$$

In case 2:

$$\begin{aligned} \frac{D_x}{E_c h^3} &\approx 0.115 \\ \frac{D_y}{E_c h^3} &\approx 0.083 \\ \frac{D_{xy}}{E_c h^3} &\approx 0.017 \\ D_x &= 1.4 D_y = 6.7 D_{xy} \end{aligned} \quad (7.1.15)$$

These cases are used for exemplification later in this report.

7.1.2 Compatibility conditions

The compatibility conditions for slabs are:

$$\begin{aligned} \frac{\partial \kappa_x}{\partial y} &= \frac{\partial \kappa_{xy}}{\partial x} \\ \frac{\partial \kappa_y}{\partial x} &= \frac{\partial \kappa_{xy}}{\partial y} \end{aligned} \quad (7.1.16)$$

If curvatures are determined from a deflection function these condition will be identically fulfilled.

A derivation may be found in [3].

7.1.3 Equilibrium equations

The equilibrium equations for a slab element are, see [3]:

$$\begin{aligned}\frac{\partial m_x}{\partial x} + \frac{\partial m_{xy}}{\partial y} - q_x &= 0 \\ \frac{\partial m_y}{\partial y} + \frac{\partial m_{xy}}{\partial x} - q_y &= 0 \\ \frac{\partial q_x}{\partial x} + \frac{\partial q_y}{\partial y} + p &= 0\end{aligned}\tag{7.1.17}$$

Eliminating the shear forces we get:

$$\frac{\partial^2 m_x}{\partial x^2} + 2 \frac{\partial^2 m_{xy}}{\partial x \partial y} + \frac{\partial^2 m_y}{\partial y^2} = -p\tag{7.1.18}$$

If this equation is fulfilled we have a statically admissible moment field.

If we introduce the constitutive equations given by formula (7.1.1) into the equilibrium equation we get:

$$D_x \frac{\partial^4 u}{\partial x^4} + 2D_{xy} \frac{\partial^4 u}{\partial x^2 \partial y^2} + D_y \frac{\partial^4 u}{\partial y^4} = p\tag{7.1.19}$$

If the bending stiffnesses are equal to the torsional stiffness we get well known differential equation:

$$\frac{\partial^4 u}{\partial x^4} + 2 \frac{\partial^4 u}{\partial x^2 \partial y^2} + \frac{\partial^4 u}{\partial y^4} = \frac{p}{D}\tag{7.1.20}$$

This is called the Lagranges equation.

7.1.4 Boundary conditions

In this paper the edge conditions are defined in Figure 7.4 (n normal to the edge).

| | | |
|-------------------------|-----------------------|--------------------------------|
| | | |
| Free edge | Simply supported edge | Fixed edge |
| Geometrical conditions: | $u = 0$ | $u = 0$ $\frac{du}{dn} = 0$ |
| Statical conditions: | $\tilde{m}_n = 0$ | |
| | $\tilde{q}_n = 0$ | |

Figure 7.4 Definition of edge conditions

The statical boundary conditions are defined using the notation of Figure 7.5.

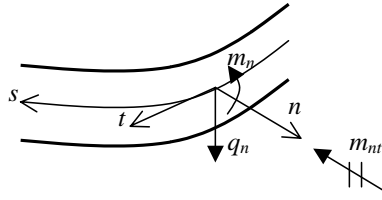


Figure 7.5 Forces along an edge.

The statical boundary conditions, also called the Kirchhoff boundary conditions, are in general (see [3]):

$$\begin{aligned}\tilde{m}_n &= m_n \\ \tilde{q}_n + \frac{\partial \tilde{m}_{nt}}{\partial s} &= q_n + \frac{\partial m_{nt}}{\partial s}\end{aligned}\quad (7.1.21)$$

If the edge is a straight line parallel say to the t -axis we may insert formulas (7.1.1) and (7.1.17) into (7.1.21). Then:

$$\tilde{m}_n = -D_n \frac{\partial^2 u}{\partial n^2} \quad (7.1.22)$$

$$\tilde{q}_n + \frac{\partial \tilde{m}_{nt}}{\partial s} = -D_n \frac{\partial^3 u}{\partial n^3} - 2D_{nt} \frac{\partial^3 u}{\partial n \partial t^2} \quad (7.1.23)$$

For a boundary parallel to the y -axis we find:

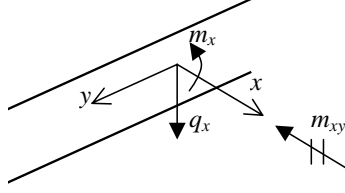


Figure 7.6 Forces along an edge.

$$\tilde{m}_x = -D_x \frac{\partial^2 u}{\partial x^2} \quad (7.1.24)$$

$$\tilde{q}_x + \frac{\partial \tilde{m}_{xy}}{\partial y} = -D_x \frac{\partial^3 u}{\partial x^3} - 2D_{xy} \frac{\partial^3 u}{\partial x \partial y^2} \quad (7.1.25)$$

7.2 Deflections of slabs with no axial force

7.2.1 Estimation of deflections using Rayleigh's principle

If we estimate the deflected form of a slab, we may use the energy equation to find an estimate of the deflections. This of course means that we do not necessarily satisfy the equilibrium equations since the sectional forces may not correspond to the load. This use of the energy equation is sometimes termed Rayleigh's principle.

The energy equation gives a relation between the load and the parameters of the deflected form.

The accuracy of the estimated deflection form is of course decisive for the accuracy of the method. In general, it is not necessary to choose a deflection form that fulfills all boundary conditions. Nevertheless, it is obvious that the most correct solution is found when both statical and geometrical boundary conditions are fulfilled. In this paper solutions, which fulfill the geometrical boundary conditions, are used. The statical boundary conditions are not fulfilled in general. The statical boundary conditions require the fulfillment of the Kirchhoff boundary conditions, formula (7.1.25). Since the ratio between the bending stiffness and the torsional stiffness is different from slab to slab it is not possible to give a general solution.

7.2.2 Beam example

In this section the method is illustrated for a beam, see Figure 7.7.

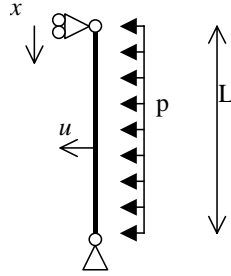


Figure 7.7 Beam

We assume a deflection in the form of a parabola given by:

$$u = \frac{4u_{\max}x(L-x)}{L^2} \quad (7.2.1)$$

The curvature is:

$$\kappa_x = -\frac{d^2u}{dx^2} = \frac{8u_{\max}}{L^2} \quad (7.2.2)$$

The work equation becomes:

$$\begin{aligned} \frac{1}{2} \int_0^L p u dx &= \frac{1}{2} \int_0^L M_x \kappa_x dx \\ \frac{1}{2} \int_0^L p u dx &= \frac{1}{2} \int_0^L D_x \kappa_x^2 dx \\ \frac{1}{2} p \frac{2}{3} u_{\max} L &= \frac{1}{2} L D_x \left(\frac{8u_{\max}}{L^2} \right)^2 \\ p &= 96 D_x \frac{u_{\max}}{L^4} \\ \text{or} \\ u_{\max} &= \frac{1}{96} \frac{p L^4}{D_x} \end{aligned} \quad (7.2.3)$$

It is evident that the assumed deflection does not fulfil the statical boundary conditions and the equilibrium equation. The deviation between the exact solution (5/384 instead of 1/96) and this solution is 20%.

If we want a deflection form that fulfils the statical boundary conditions we may take:

$$u = u_{\max} \sin\left(\pi \frac{x}{L}\right) \quad (7.2.4)$$

The work equation gives:

$$p = \frac{\pi^5}{4} D_x \frac{u_{\max}}{L^4}$$

or

$$u_{\max} = \frac{4}{\pi^5} \frac{p L^4}{D_x} \quad (7.2.5)$$

In this case the deviation is less than 1%.

A deviation of this order is acceptable for all practical calculations.

7.2.3 Rectangular slab simply supported at all sides

In this case we consider a rectangular slab simply supported at all sides and loaded with a uniformly distributed load p , see Figure 7.8.

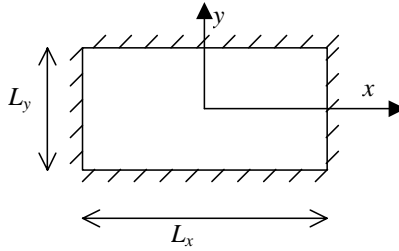


Figure 7.8 Rectangular slab simply supported at all sides

We estimate a deflection function given by:

$$u = u_{\max} \sin \left(\frac{\left(y + \frac{L_y}{2} \right) \pi}{L_y} \right) \sin \left(\frac{\left(x + \frac{L_x}{2} \right) \pi}{L_x} \right) \quad (7.2.6)$$

The deflected form is illustrated in Figure 7.9.

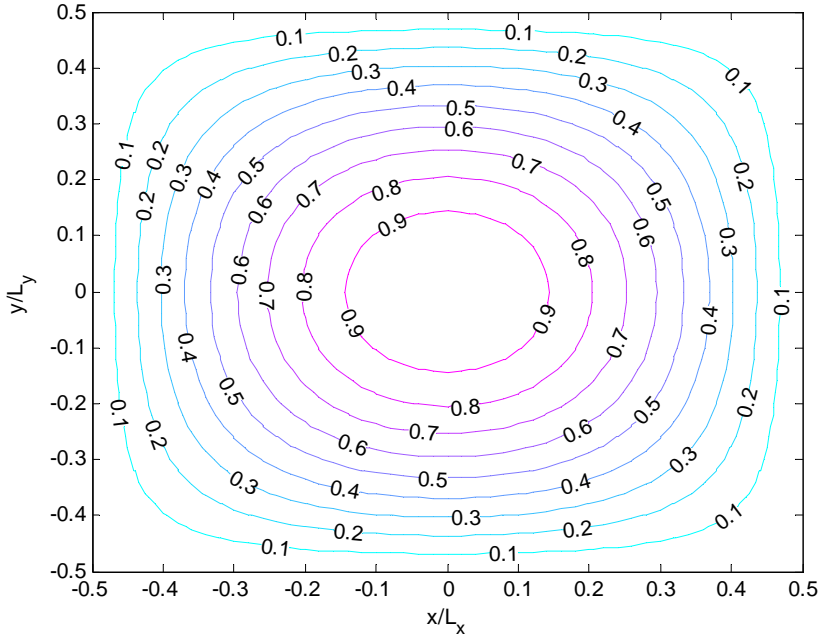


Figure 7.9 Deflection over maximum deflection.

It is seen that the geometrical boundary conditions are fulfilled:

$$u\left(x=\frac{L_x}{2}\right) = u\left(x=-\frac{L_x}{2}\right) = u\left(y=\frac{L_y}{2}\right) = u\left(y=-\frac{L_y}{2}\right) = 0 \quad (7.2.7)$$

In this case we should have a bending moment of zero along the edges in order to fulfil the statical boundary conditions. These are fulfilled if:

$$\kappa_x\left(x=\frac{L_x}{2}\right) = \kappa_x\left(x=-\frac{L_x}{2}\right) = \kappa_y\left(y=\frac{L_y}{2}\right) = \kappa_y\left(y=-\frac{L_y}{2}\right) = 0 \quad (7.2.8)$$

Using the energy or work equation we get:

$$\begin{aligned} \frac{1}{2} \int_{-\frac{L_y}{2}}^{\frac{L_y}{2}} \int_{-\frac{L_x}{2}}^{\frac{L_x}{2}} p u dxdy &= \frac{1}{2} \int_{-\frac{L_y}{2}}^{\frac{L_y}{2}} \int_{-\frac{L_x}{2}}^{\frac{L_x}{2}} (M_x \kappa_x + M_y \kappa_y + 2M_{xy} \kappa_{xy}) dxdy \\ \frac{1}{2} \int_{-\frac{L_y}{2}}^{\frac{L_y}{2}} \int_{-\frac{L_x}{2}}^{\frac{L_x}{2}} p u dxdy &= \frac{1}{2} \int_{-\frac{L_y}{2}}^{\frac{L_y}{2}} \int_{-\frac{L_x}{2}}^{\frac{L_x}{2}} (D_x \kappa_x^2 + D_y \kappa_y^2 + 2D_{xy} \kappa_{xy}^2) dxdy \\ \frac{2pu_{\max} L_x L_y}{\pi^2} &= \frac{1}{8} \frac{u_{\max}^2 \pi^4}{L_y^3 L_x^3} (D_x L_y^4 + L_x^4 D_y + 2D_{xy} L_x^2 L_y^2) \Leftrightarrow \\ p &= \frac{u_{\max} \pi^6}{16} \frac{D_x L_y^4 + L_x^4 D_y + 2D_{xy} L_x^2 L_y^2}{L_y^4 L_x^4} \end{aligned} \quad (7.2.9)$$

7.2.4 Rectangular slab simply supported at three sides and one free edge

We now consider a rectangular slab simply supported at three sides, one free edge and loaded with a uniformly distributed load p , see Figure 7.10.

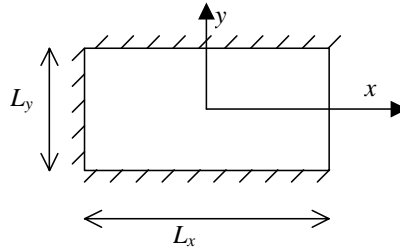


Figure 7.10 Rectangular slab simply supported at three sides

In this case, we estimate a deflection function given by:

$$u = u_{\max} \sin \left(\frac{\left(y + \frac{L_y}{2} \right) \pi}{L_y} \right) \sin \left(\frac{\left(x + \frac{L_x}{2} \right) \pi}{2L_x} \right) \quad (7.2.10)$$

The deflected form is illustrated in Figure 7.11

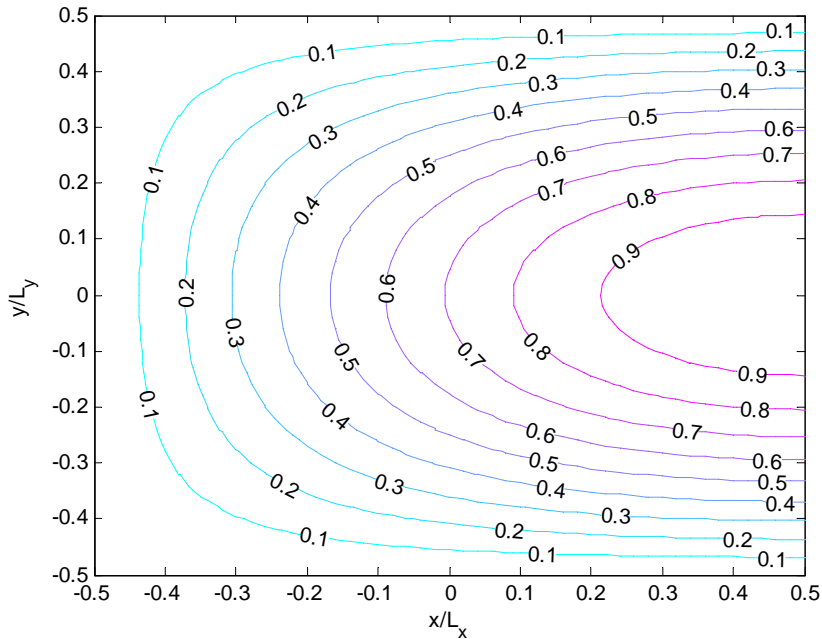


Figure 7.11 Deflection over maximum deflection.

It is seen that the geometrical boundary conditions are fulfilled:

$$\begin{aligned} u_{\left(x=-\frac{L_x}{2}\right)} &= u_{\left(y=-\frac{L_y}{2}\right)} = u_{\left(y=\frac{L_y}{2}\right)} = 0 \\ u_{\left(x=\frac{L_x}{2}\right)} &= u_{\max} \sin\left(\frac{(2y + L_y)\pi}{2L_y}\right) \end{aligned} \quad (7.2.11)$$

In this case the statical boundary conditions are not fulfilled since we have:

$$\begin{aligned} \kappa_{x\left(x=-\frac{L_x}{2}\right)} &= \kappa_{y\left(y=-\frac{L_y}{2}\right)} = \kappa_{y\left(y=\frac{L_y}{2}\right)} = 0 \\ \kappa_{x\left(x=\frac{L_x}{2}\right)} &= -\frac{\pi^2}{4} \frac{u_{\max} \sin\left(\frac{(2y + L_y)\pi}{2L_y}\right)}{L_x^2} \end{aligned} \quad (7.2.12)$$

The moment $m_{x(x=1/2L_y)}$ becomes:

$$m_{x\left(x=\frac{L_x}{2}\right)} = -\frac{D_x \pi^2}{4} \frac{u_{\max} \sin\left(\frac{(2y + L_y)\pi}{2L_y}\right)}{L_x^2} \quad (7.2.13)$$

which means that the boundary condition for m_x is not fulfilled. Further the Kirchhoff boundary conditions (7.1.25) along the free edge are not fulfilled.

Using the work equation we get:

$$\begin{aligned} \frac{1}{2} \int_{-\frac{L_y}{2}}^{\frac{L_y}{2}} \int_{-\frac{L_x}{2}}^{\frac{L_x}{2}} p u dxdy &= \frac{1}{2} \int_{-\frac{L_y}{2}}^{\frac{L_y}{2}} \int_{-\frac{L_x}{2}}^{\frac{L_x}{2}} (M_x \kappa_x + M_y \kappa_y + 2M_{xy} \kappa_{xy}) dxdy \Leftrightarrow \\ p &= \frac{u_{\max} \pi^6}{256} \frac{D_x L_y^4 + 16L_x^4 D_y + 8D_{xy} L_x^2 L_y^2}{L_y^4 L_x^4} \end{aligned} \quad (7.2.14)$$

We now assume another deflection form given by:

$$u = u_{\max} \sin\left(\frac{\left(y + \frac{L_y}{2}\right)\pi}{L_y}\right) \sin\left(\frac{\left(x + \frac{L_x}{2}\right)\pi}{L_x}\right) \quad (7.2.15)$$

The deflected form is illustrated in Figure 7.12.

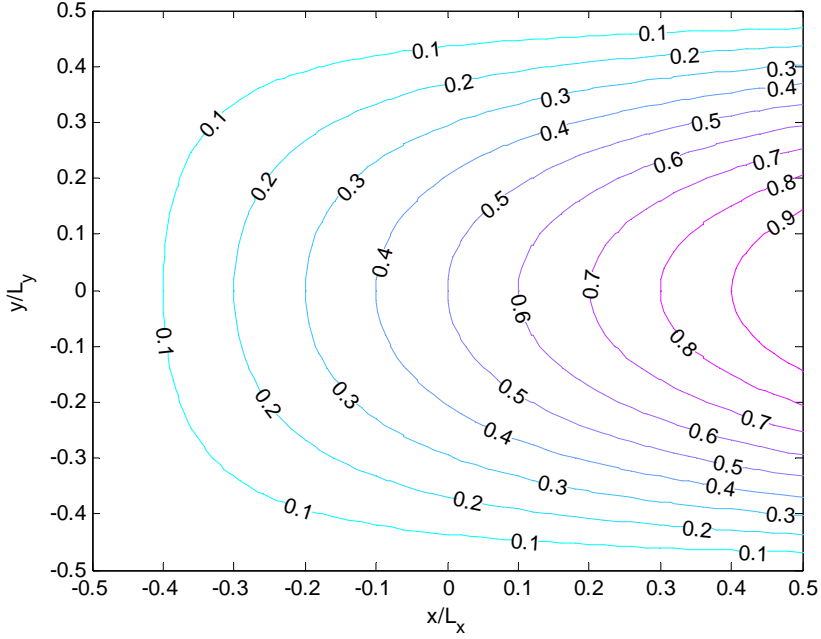


Figure 7.12 Deflection over maximum deflection.

It appears that the statical boundary condition (7.1.25) is still not fulfilled. However, this deflection form leads to no bending moments along the edges and is therefore more accurate. In this case we find the following relation between p and u_{\max} .

$$p = \frac{u_{\max} \pi^3}{6} \frac{6D_{xy} L_y^2 + \pi^2 L_x^2 D_y}{L_x^2 L_y^4} \quad (7.2.16)$$

Notice that in this case the bending stiffness in the x -direction has no influence.

As a third possibility consider a deflection given by, see Figure 7.13:

$$u = u_{\max} \frac{3}{4} \sqrt{2} \sqrt{3} \sin \left(\frac{\left(y + \frac{L_y}{2} \right) \pi}{L_y} \right) \sin \left(\frac{\left(x + \frac{L_x}{2} \right) \text{Arc tan}(\sqrt{2})}{L_x} \right)^3 \quad (7.2.17)$$

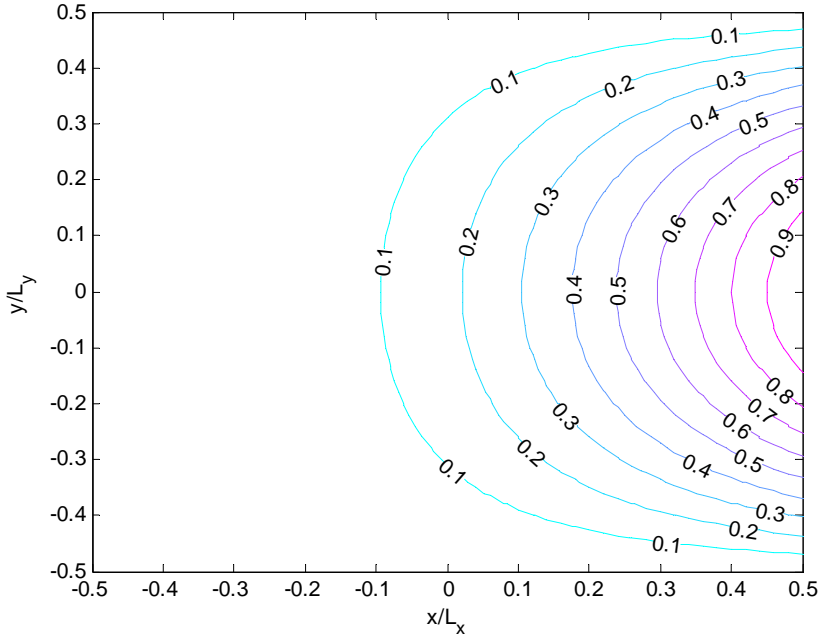


Figure 7.13 Deflection over maximum deflection.

Still the static boundary conditions are not fulfilled in general but the bending moment m_x at the free edge is zero.

We find the following relation between p and u_{max} .

$$p = \frac{u_{max}}{512} \frac{\left(405\pi^4 \text{Arc tan}\left(\sqrt{2}\right) D_y L_x^4 - 227\pi^4 \sqrt{2} L_x^4 D_y \right.}{L_x^4 L_y^4 (-4\sqrt{3} + 9)} \left. + 1458\pi^2 \left(\text{Arc tan}\left(\sqrt{2}\right) \right)^3 D_{xy} L_x^2 L_y^2 - 126\pi^2 \sqrt{2} \left(\text{Arc tan}\left(\sqrt{2}\right) \right)^2 D_{xy} L_x^2 L_y^2 \right. \left. - 891\sqrt{2} \left(\text{Arc tan}\left(\sqrt{2}\right) \right)^4 D_x L_y^4 + 3645 \left(\text{Arc tan}\left(\sqrt{2}\right) \right)^5 D_x L_y^4 \right) \quad (7.2.18)$$

$$p \approx u_{max} \frac{(46,6 D_y L_x^4 + 79,4 D_{xy} L_x^2 L_y^2 + 13,4 D_x L_y^4)}{L_x^4 L_y^4}$$

If we compare this solution with the previous solution we notice that the last solution involves the bending stiffness in the x –direction. Whether this is relevant or not depends on the ratio between the side lengths. If L_y is very large compared to L_x it is logical that the bending stiffness in the x - direction will have a small effect since the slab is unable to carry any substantial load in that direction. The other extreme is when L_x is very large compared to L_y and in this case the slab will of course be able to carry a substantial part of the load in the x –direction.

7.2.5 Rectangular slab fixed at all sides

In this case we consider a rectangular slab fixed at all sides and loaded with a uniformly distributed load p , see Figure 7.14.

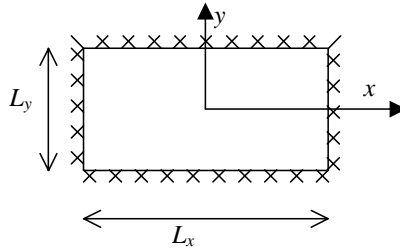


Figure 7.14 Rectangular slab fixed at all sides

We estimate a deflection function given by, see Figure 7.15:

$$u = u_{\max} \sin \left(\frac{\left(y + \frac{L_y}{2} \right) \pi}{L_y} \right)^2 \sin \left(\frac{\left(x + \frac{L_x}{2} \right) \pi}{L_x} \right)^2 \quad (7.2.19)$$

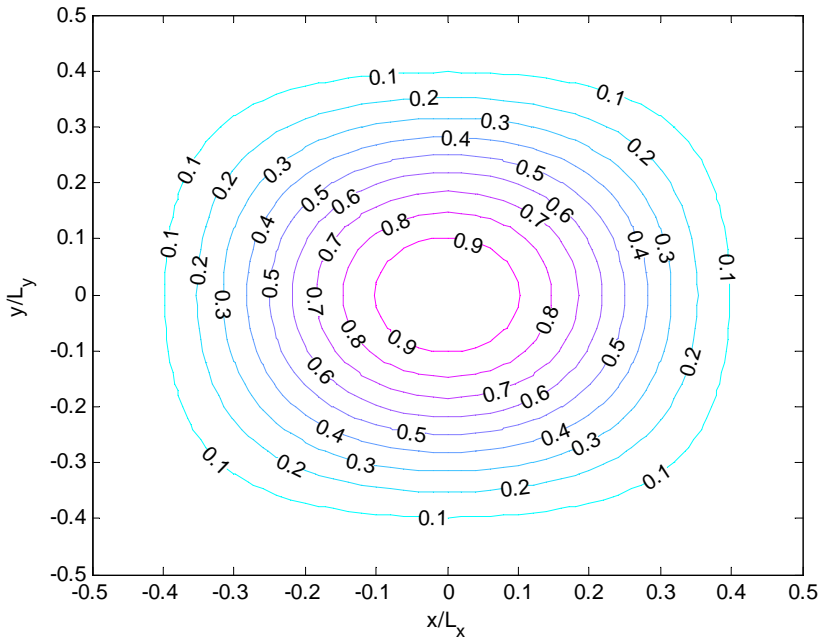


Figure 7.15 Deflection over maximum deflection

In this case it may be shown that both the geometrical and statical boundary conditions are fulfilled.

Using the work equation we get:

$$p = u_{\max} \pi^4 \frac{3D_x L_y^4 + 3L_x^4 D_y + 2D_{xy} L_x^2 L_y^2}{L_y^4 L_x^4} \quad (7.2.20)$$

7.2.6 Rectangular slab with two adjacent sides fixed and two sides free

In this case we consider a rectangular slab fixed at two sides next to each other and loaded with a uniformly distributed load p , see Figure 7.16.

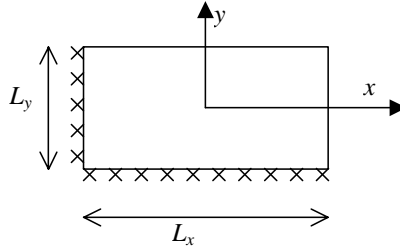


Figure 7.16 Rectangular slab fixed at two sides and with two sides free.

In this case, we may estimate a deflection function given by, see Figure 7.15:

$$u = u_{\max} 4 \sin \left(\frac{\left(y + \frac{L_y}{2} \right) \pi}{4L_y} \right)^2 \sin \left(\frac{\left(x + \frac{L_x}{2} \right) \pi}{4L_x} \right)^2 \quad (7.2.21)$$

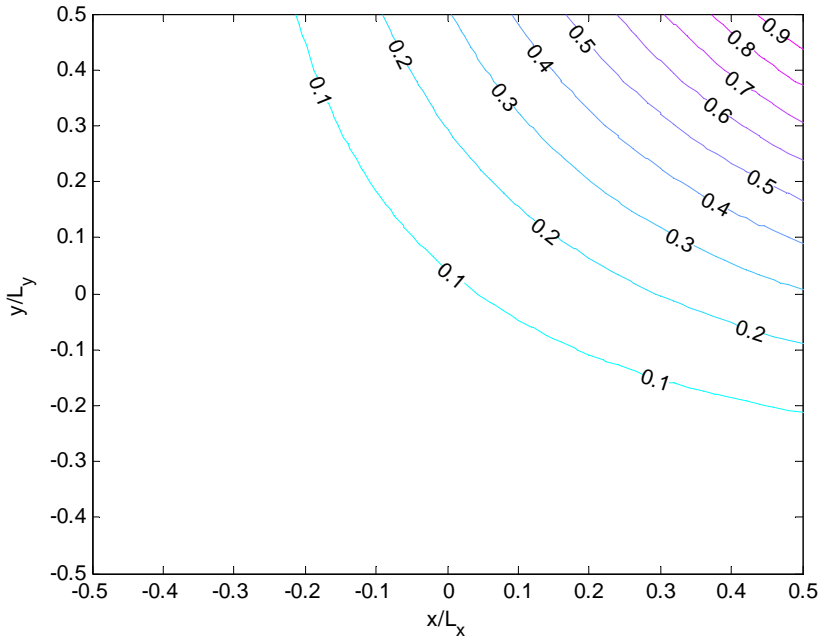


Figure 7.17 Deflection over maximum deflection

It may be shown that the geometrical boundary condition are fulfilled. The statical boundary condition (7.1.25) is not fulfilled.

Using the work equation we get:

$$p \approx u_{\max} \frac{5, 2D_x L_y^4 + 5, 2L_x^4 D_y + 23, 1D_{xy} L_x^2 L_y^2}{L_y^4 L_x^4} \quad (7.2.22)$$

7.2.7 Rectangular slab with two adjacent sides simply supported and two sides free

In this case we consider a rectangular slab simply supported at two sides next to each other and loaded with a uniformly distributed load p see Figure 7.18.

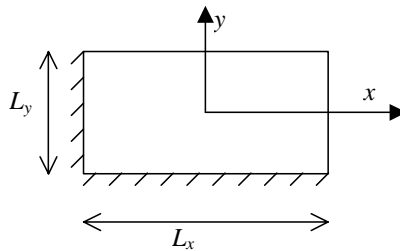


Figure 7.18 Rectangular slab simply supported at two sides, two sides free.

In this case, we may estimate a deflection function given by, see Figure 7.19:

$$u = u_{\max} \frac{27}{8} \sin \left(\frac{\left(y + \frac{L_y}{2} \right) \text{Arc tan}(\sqrt{2})}{L_y} \right)^3 \sin \left(\frac{\left(x + \frac{L_x}{2} \right) \text{Arc tan}(\sqrt{2})}{L_x} \right)^3 \quad (7.2.23)$$

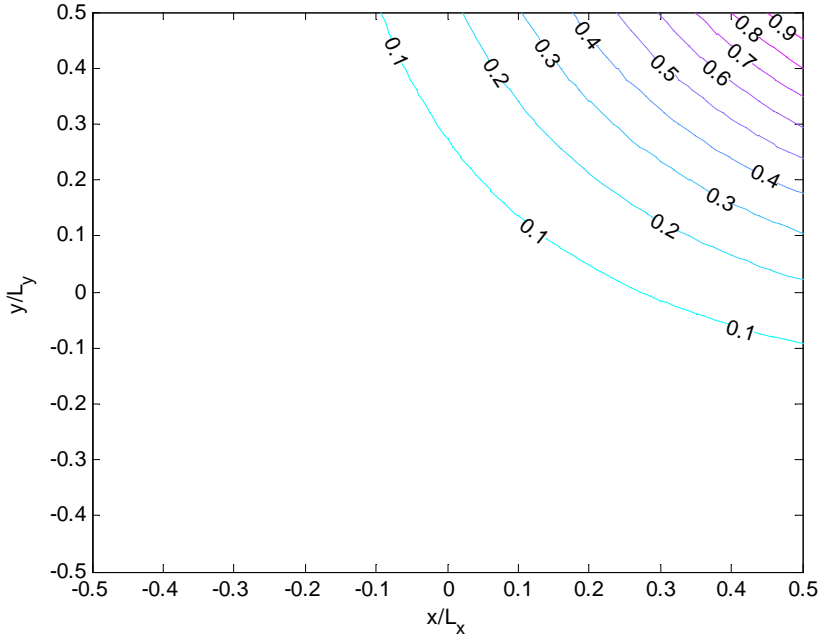


Figure 7.19 Deflection over maximum deflection

It may be shown that the geometrical boundary conditions are fulfilled. The statical boundary condition (7.1.25) is not fulfilled.

Using the work equation we get:

$$p = u_{\max} \frac{10.4D_x L_y^4 + 10.4L_x^4 D_y + 52.4D_{xy} L_x^2 L_y^2}{L_y^4 L_x^4} \quad (7.2.24)$$

7.2.8 Exemplification of deflection calculations

In order to evaluate the influence of the torsional stiffness and the influence the position of the reinforcement we show the result of some examples.

In section 7.1.1.1 it was demonstrated that if the reinforcement is placed close to the faces the torsional stiffness is of the order one third of the bending stiffness and if the reinforcement is placed in the centre the torsional stiffness is the same as the bending stiffness.

If we consider a square slab and assume that the reinforcement is isotropic we may compare the maximum deflection for a given load using the formulas above.

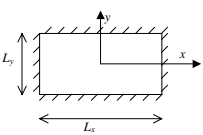
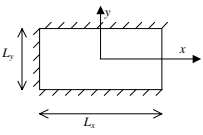
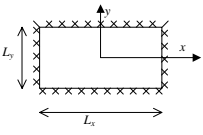
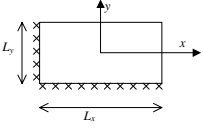
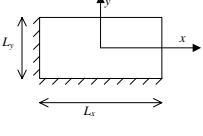
| $L_x/L_y=1$, Isotropic reinforcement | Formula | Case 1. Reinforcement placed in the centre. ($D_{xy}=D_x=D_y$) | Case 2. Reinforcement placed close to the faces. ($3D_{xy}=D_x=D_y$) | $\frac{p_{case1}}{p_{case2}}$ |
|---|----------|--|--|-------------------------------|
|  | (7.2.9) | $p = 240.3 \frac{u_{max} D_x}{L_x^4}$ | $p = 160.2 \frac{u_{max} D_x}{L_x^4}$ | 1.5 |
|  | (7.2.14) | $p = 93.9 \frac{u_{max} D_x}{L_x^4}$ | $p = 73.9 \frac{u_{max} D_x}{L_x^4}$ | 1.3 |
| | (7.2.16) | $p = 82.0 \frac{u_{max} D_x}{L_x^4}$ | $p = 61.3 \frac{u_{max} D_x}{L_x^4}$ | 1.3 |
| | (7.2.18) | $p = 139.4 \frac{u_{max} D_x}{L_x^4}$ | $p = 86.5 \frac{u_{max} D_x}{L_x^4}$ | 1.6 |
|  | (7.2.20) | $p = 779.3 \frac{u_{max} D_x}{L_x^4}$ | $p = 649.4 \frac{u_{max} D_x}{L_x^4}$ | 1.2 |
|  | (7.2.22) | $p = 33.5 \frac{u_{max} D_x}{L_x^4}$ | $p = 18.1 \frac{u_{max} D_x}{L_x^4}$ | 1.9 |
|  | (7.2.24) | $p = 73.2 \frac{u_{max} D_x}{L_x^4}$ | $p = 38.3 \frac{u_{max} D_x}{L_x^4}$ | 1.9 |

Table 7.1 Relation between load and deflection for different slabs.

Table 7.1 demonstrates the effect of a change in the ratio between the bending stiffness and the torsional stiffness. In is clear that the effect is most pronounced for the slabs with two free adjacent sides. This is to be expected since the slab “carries” the load mainly in torsion.

Also a slab simply supported at all four sides is quite affected whereas the slab fixed at all four sides is much less affected, which is due to the fact that the torsional moments are small.

For the slab simply supported at 3 sides and one free, 3 formulas for different deflection forms are used as described in section 7.2.4. Formula (7.2.14) is a deflection form that leads to bending moments along the free edge and thus it does not lead to a particularly good solution. However, it is seen that even though this deflection form is not accurate the result does not deviate that much from the other two solutions where bending moments along the free edge are zero.

As for the two other solutions the difference is here whether the deflection varies linearly or sinusoidal in the x -direction. It is seen that for the present ratio between the side lengths a linear variation leads to a lower stiffness. Since we are dealing with upper bound solutions the solution with the lower stiffness is to be preferred.

If the ratio between the side lengths, L_x/L_y , is more than approximately 3, the sinusoidal deflection form will lead to a better result.

7.3 Stability of slabs loaded with axial force

If a slab is subjected to axial forces in one or two directions the maximum load may be governed by instability.

If the slab is subjected to axial forces (compressive) in both directions the slab initially will be uncracked, and the stiffness may be calculated for uncracked concrete.

If the reinforcement is placed in the centre and the bending stiffnesses are the same as the torsional stiffness, the calculations may be carried out according to the standard theory of elastic stability. In this case the solutions described in for example [3] or [15] may be used directly. The nonlinear stress-strain relation for concrete may be taken into account by letting the modulus of elasticity depend on the normal force, cf. the standard theory for concrete columns.

In all other cases the load at instability must be found in a way that takes into account the difference in the stiffnesses. In this report the use of Bryan's equation is described.

Bryan's equation for a slab is (see [12], [3]):

$$\begin{aligned}
 0 = & \frac{1}{2} \iint \left(D_x \left(\frac{\partial^2 u}{\partial x^2} \right)^2 + D_y \left(\frac{\partial^2 u}{\partial y^2} \right)^2 + 2D_{xy} \left(\frac{\partial^2 u}{\partial x \partial y} \right)^2 \right) dx dy \\
 & + \frac{1}{2} \iint \left(n_x \left(\frac{\partial u}{\partial x} \right)^2 + n_y \left(\frac{\partial u}{\partial y} \right)^2 + 2n_{xy} \frac{\partial u}{\partial x} \frac{\partial u}{\partial y} \right) dx dy
 \end{aligned} \tag{7.3.1}$$

Here n_x and n_y are positive for tensile forces. The sign convention for n_{xy} follows the coordinate system in the usual way.

The method is to estimate a deflection form and then use Bryan's equation to find the load at instability. The method is demonstrated in the next section.

7.3.1 Rectangular slab simply supported at all sides

In this case we consider a rectangular slab simply supported at all sides. The slab is loaded by a uniformly distributed load p and there may be axial forces in one or two directions, see Figure 7.20.

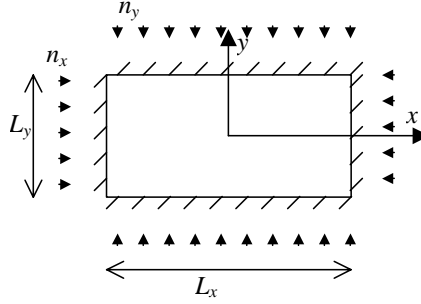


Figure 7.20 Rectangular slab simply supported at all sides

We estimate the same deflection function as in the case with no axial forces:

$$u = u_{\max} \sin \left(\frac{\left(y + \frac{L_y}{2} \right) \pi}{L_y} \right) \sin \left(\frac{\left(x + \frac{L_x}{2} \right) \pi}{L_x} \right) \tag{7.3.2}$$

Inserting into Bryan's equation we get:

$$n_x = \pi^2 \frac{D_x L_y^4 + L_x^4 D_y + D_{xy} L_x^2 L_y^2 - L_x^4 L_y^2 \frac{n_y}{\pi^2}}{L_x^2 L_y^4} \tag{7.3.3}$$

Similar calculations are made without any further comments for other slabs in the following sections.

7.3.2 Rectangular slab simply supported at three sides and one free edge

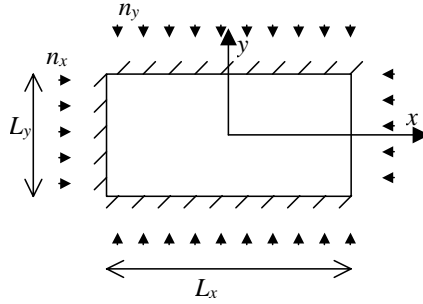


Figure 7.21 Rectangular slab simply supported at three sides

Deflection function:

$$u = u_{\max} \sin \left(\frac{\left(y + \frac{L_y}{2} \right) \pi}{L_y} \right) \sin \left(\frac{\left(x + \frac{L_x}{2} \right)}{L_x} \right) \quad (7.3.4)$$

Bryan's equation:

$$n_x = \frac{\pi^2}{3} \frac{3D_{xy}L_y^2 + D_y\pi^2L_x^2 - L_y^2n_yL_x^2}{L_y^4} \quad (7.3.5)$$

Deflection function:

$$u = u_{\max} \frac{3}{4} \sqrt{2} \sqrt{3} \sin \left(\frac{\left(y + \frac{L_y}{2} \right) \pi}{L_y} \right) \sin \left(\frac{\left(x + \frac{L_x}{2} \right) \text{Arc tan}(\sqrt{2})}{L_x} \right)^3 \quad (7.3.6)$$

Bryan's equation:

$$n_x = \frac{3.34D_xL_y^4 + 11.58D_yL_x^4 + 9.87D_{xy}L_x^2L_y^2 - 1.17L_x^4L_y^2n_y}{L_y^4L_x^2} \quad (7.3.7)$$

7.3.3 Rectangular slab fixed at all sides

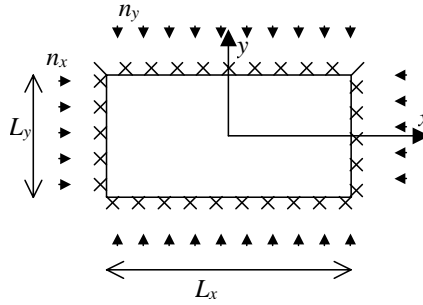


Figure 7.22 Rectangular slab fixed at all sides

Deflection function:

$$u = u_{\max} \sin \left(\frac{\left(y + \frac{L_y}{2} \right) \pi}{L_y} \right)^2 \sin \left(\frac{\left(x + \frac{L_x}{2} \right) \pi}{L_x} \right)^2 \quad (7.3.8)$$

Bryan's equation:

$$n_x = \frac{\pi^2}{3} \frac{12D_x L_y^4 + 12D_y L_x^4 + 4D_{xy} L_x^2 L_y^2 - 3L_x^4 L_y^2 \frac{n_y}{\pi^2}}{L_x^2 L_y^4} \quad (7.3.9)$$

7.3.4 Rectangular slab with two adjacent sides fixed and two sides free

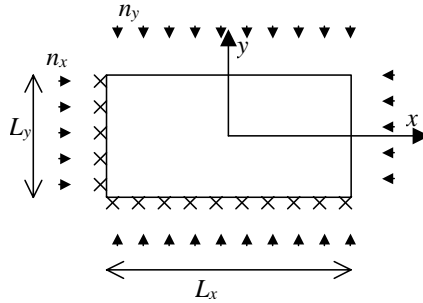


Figure 7.23 Rectangular slab fixed at two sides, two sides free

Deflection function:

$$u = u_{\max} 4 \sin \left(\frac{\left(y + \frac{L_y}{2} \right) \pi}{4L_y} \right)^2 \sin \left(\frac{\left(x + \frac{L_x}{2} \right) \pi}{4L_x} \right)^2 \quad (7.3.10)$$

Bryan's equation:

$$n_x = \frac{5.44D_{xy}L_x^2L_y^2 - L_x^4L_y^2n_y + 2.47D_yL_x^4 + 2.47D_xL_y^4}{L_x^2L_y^4} \quad (7.3.11)$$

7.3.5 Rectangular slab with two adjacent sides simply supported and two sides free

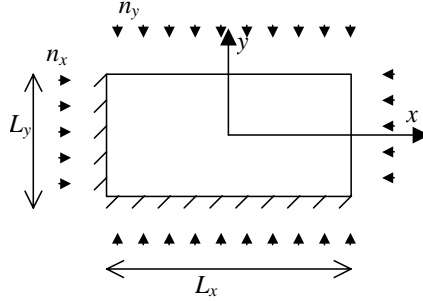


Figure 7.24 Rectangular slab simply supported at two sides, two sides free

Deflection function:

$$u = u_{\max} \frac{27}{8} \sin \left(\frac{\left(y + \frac{L_y}{2} \right) \text{Arc tan}(\sqrt{2})}{L_y} \right)^3 \sin \left(\frac{\left(x + \frac{L_x}{2} \right) \text{Arc tan}(\sqrt{2})}{L_x} \right)^3 \quad (7.3.12)$$

Bryan's equation:

$$n_x = \frac{8.41D_{xy}L_x^2L_y^2 - L_x^4L_y^2n_y + 3.34D_yL_x^4 + 3.34D_xL_y^4}{L_x^2L_y^4} \quad (7.3.13)$$

7.3.6 Exemplification of stability calculations

Again we evaluate the influence of the torsional stiffness and the influence the position of the reinforcement through some examples.

We consider a square slab subjected to the same axial force in both directions and assume that the reinforcement is isotropic. The stiffnesses in this situation are given by formulas (7.1.12) and (7.1.13). Using the formulas from the previous sections we get the results in Table 7.2.

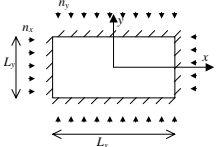
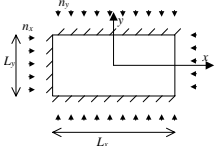
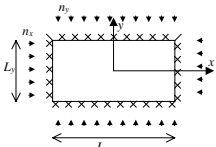
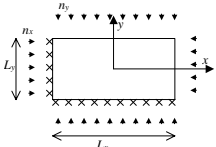
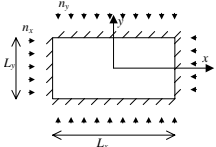
| $L_x/L_y=1$, Isotropic reinforcement, $n_x/n_y=1$ | Formula | Case 1. Reinforcement placed in the centre. Formula (7.1.12) ($D_{xy}=D_x=D_y$) | Case 2. Reinforcement placed close to the faces. Formula (7.1.13) ($1.4D_{xy}=D_x=D_y$) | $\frac{n_{x,case1}}{n_{x,case2}}$ |
|---|--------------------|--|---|-----------------------------------|
|  | (7.3.3) | $n_x = 14.8 \frac{D_x}{L_x^2}$ | $n_x = 13.4 \frac{D_x}{L_x^2}$ | 1.1 |
|  | (7.3.5) (7.3.7) | $n_x = 9.9 \frac{D_x}{L_x^2}$ $n_x = 11.4 \frac{D_x}{L_x^2}$ | $n_x = 9.2 \frac{D_x}{L_x^2}$ $n_x = 10.1 \frac{D_x}{L_x^2}$ | 1.1 1.1 |
|  | (7.3.9) | $n_x = 46.1 \frac{D_x}{L_x^2}$ | $n_x = 44.2 \frac{D_x}{L_x^2}$ | 1.0 |
|  | (7.3.11) | $n_x = 5.2 \frac{D_x}{L_x^2}$ | $n_x = 4.4 \frac{D_x}{L_x^2}$ | 1.2 |
|  | (7.3.13) | $n_x = 7.5 \frac{D_x}{L_x^2}$ | $n_x = 6.3 \frac{D_x}{L_x^2}$ | 1.2 |

Table 7.2 Load at instability for different cases and slabs.

Table 7.2 demonstrates the effect of a change in the ratio between the bending stiffness and the torsional stiffness. As expected the effect is most pronounced for slabs with two free adjacent sides.

It is seen that if the slab is subjected to compressive axial force in two directions, the position of the reinforcement does not influence the stability load significantly.

It should be noted that for the slab simply supported at three sides and with one free edge the lower value of the axial force at instability should be used since we are dealing with upper bound solutions.

We now consider a square slab subjected to axial force in one direction only and assume that the reinforcement is isotropic. The stiffnesses in this situation are given by formulas (7.1.14) and (7.1.15). Using the formulas from the previous sections we get the results shown in Table 7.3.

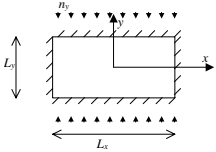
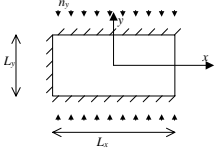
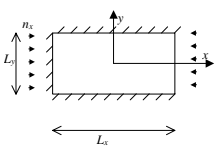
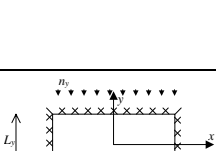
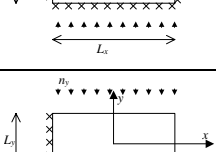
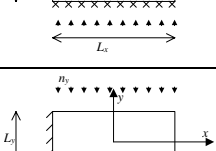
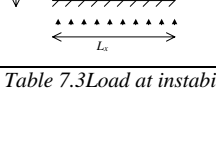

| $L_x/L_y=1$, Isotropic reinforcement, $n_x=0$ | Formula | Case 1. Reinforcement placed in the centre. Formula (7.1.14) ($D_y=4.9D_x= 4.9D_{xy}$) | Case 2. Reinforcement placed close to the faces. Formula (7.1.15) ($D_y=1.4D_x= 6.7D_{xy}$) | $\frac{n_{x,case1}}{n_{x,case2}}$ |
|---|----------|---|--|-----------------------------------|
|  | (7.3.3) | $n_y = 13.9 \frac{D_y}{L_y^2}$ | $n_y = 18.4 \frac{D_y}{L_y^2}$ | 0.8 |
|  | (7.3.5) | $n_x = 2.6 \frac{D_y}{L_y^2}$ | $n_y = 7.5 \frac{D_y}{L_y^2}$ | 0.4 |
|  | (7.3.7) | $n_y = 6.6 \frac{D_y}{L_y^2}$ | $n_y = 11.2 \frac{D_y}{L_y^2}$ | 0.6 |
|  | (7.3.5) | ($D_x=4.9D_y= 4.9D_{xy}$) | ($D_x=1.4D_y= 6.7D_{xy}$) | |
|  | (7.3.7) | $n_x = 34.5 \frac{D_x}{L_y^2}$ | $n_x = 33.9 \frac{D_x}{L_y^2}$ | 1.0 |
|  | | $n_x = 14.3 \frac{D_x}{L_y^2}$ | $n_x = 15.4 \frac{D_x}{L_y^2}$ | 0.9 |
|  | (7.3.9) | $n_y = 50.2 \frac{D_y}{L_y^2}$ | $n_y = 69.6 \frac{D_y}{L_y^2}$ | 0.72 |
|  | (7.3.11) | $n_y = 4.1 \frac{D_y}{L_y^2}$ | $n_y = 5.1 \frac{D_y}{L_y^2}$ | 0.8 |
| | (7.3.13) | $n_y = 5.7 \frac{D_y}{L_y^2}$ | $n_y = 7.0 \frac{D_y}{L_y^2}$ | 0.8 |

Table 7.3 Load at instability for different cases and slabs.

In these cases neither the ratio between bending stiffnesses and the torsional stiffness nor the ratio between the two bending stiffnesses is the same. It is seen that the change in the ratio between the bending stiffnesses gives the most dominant effect.

As expected, the slabs with two sides free are not as affected by a difference between the bending stiffnesses as the other ones.

7.4 Deflections of slabs with axial force

If a slab is subjected to both axial forces and transverse load both types of loads must be taken into account in the work equation. The work equation becomes:

$$\begin{aligned} \frac{1}{2} \iint p u d x d y &= \frac{1}{2} \iint \left(D_x \left(\frac{\partial^2 u}{\partial x^2} \right)^2 + D_y \left(\frac{\partial^2 u}{\partial y^2} \right)^2 + 2 D_{xy} \left(\frac{\partial^2 u}{\partial x \partial y} \right)^2 \right) d x d y \\ &- \frac{1}{2} \iint \left(n_x \left(\frac{\partial u}{\partial x} \right)^2 + n_y \left(\frac{\partial u}{\partial y} \right)^2 + 2 n_{xy} \frac{\partial u}{\partial x} \frac{\partial u}{\partial y} \right) d x d y \end{aligned} \quad (7.4.1)$$

Notice that in this equation n_x and n_y are positive for tension.

For such slabs there are some further complications. First of all, the stiffnesses change as a function of the loads and as a function of the position in the slab. The stiffnesses are functions of the ratio between the axial forces and the moments. Since the moments change throughout the slab the stiffnesses will also change throughout the slab.

For most practical purposes a reasonable estimate of the behaviour of the slab is sufficient. Therefore we will demonstrate how to carry out the calculations using only one set of stiffnesses throughout the slab equal to the lower values of the actual stiffnesses. The procedure is demonstrated in the following section.

7.4.1 Rectangular slab simply supported at four sides loaded with an axial force in one direction

In this section we consider a slab simply supported at all sides. The slab is loaded by an axial force in one direction only and a uniformly distributed transverse load, see Figure 7.25.

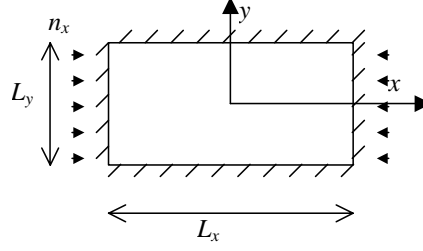


Figure 7.25 Rectangular slab simply supported at all sides. Uniform load and axial force in one direction.

The deflection form is given by formula (7.3.2). The work equation, formula (7.4.1), leads to the following relation between the axial force, maximum deflection and transverse load:

$$p = \frac{1}{16} u_{\max} \pi^4 \frac{\pi^2 D_x L_y^4 + \pi^2 L_x^4 D_y + 2\pi^2 D_{xy} L_x^2 L_y^2 - L_y^4 L_x^2 n_x}{L_x^4 L_y^4} \quad (7.4.2)$$

We have, as mentioned above, assumed that the stiffnesses are the same throughout the slab.

This assumption is correct regarding the bending stiffness in the y -direction and it is also correct for the torsional stiffness if we use the constitutive equations described previously in section 7.1.1.

However, the assumption is not correct regarding the bending stiffness in the x -direction. This bending stiffness is estimated by using the stiffness at the point of maximum bending moment in the x -direction. This point is determined by:

$$\left. \begin{aligned} \frac{d\kappa_x}{dx} = 0 &\Rightarrow x = 0 \\ \frac{d\kappa_x}{dy} = 0 &\Rightarrow y = 0 \end{aligned} \right\} \Rightarrow \kappa_{x,\max} = \frac{\pi^2 u_{\max}}{L_x^2} \quad (7.4.3)$$

Thus the bending stiffness in the centre of the slab is used throughout the slab. Formula (7.4.3) may also be used to determine the relation between bending moment, stiffness and maximum deflection. This is:

$$m_{x,\max} = D_{x,\max} \frac{\pi^2 u_{\max}}{L_x^2} \Leftrightarrow u_{\max} = \frac{L_x^2 m_{x,\max}}{\pi^2 D_{x,\max}} \quad (7.4.4)$$

The calculation of an interaction diagram between the axial force and the transverse load may now be done in the following way:

For a given axial load a maximum bending moment in the x -direction is assumed, and by using the constitutive equations described in section 7.1.1 the stiffnesses are determined.

Then the maximum deflection may be determined by formula (7.4.4). Knowing the maximum deflection, formula (7.4.2) may then be used to determine the transverse load. By varying the bending moment for different constant axial forces diagrams like those shown in Figure 7.26 and Figure 7.27 are obtained.

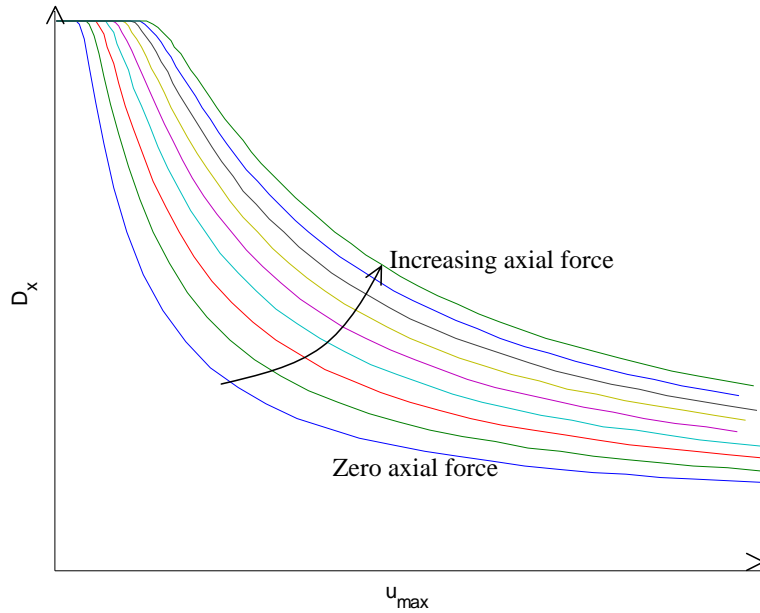


Figure 7.26 Bending stiffness as a function of maximum deflection for different axial loads.

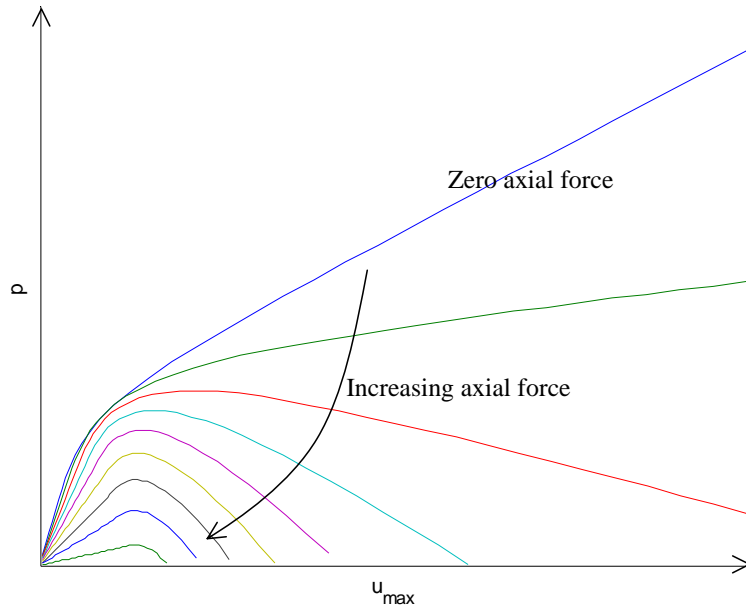


Figure 7.27 Transverse load as a function of maximum deflection for different axial loads.

Using Figure 7.27 the maximum transverse load may be found for a given axial force as illustrated in Figure 7.28. It is evident that if the axial force is sufficiently low the load continues to increase as the maximum deflection increases. In such cases, we do not have failure by instability and these points are therefore left out in Figure 7.28. We may still use the formulas to determine the relation between axial force, maximum deflection and transverse load. The failure will be a material failure. In such case, the load carrying capacity may be determined by introducing maximum stresses.

A short description of the procedure for may be seen in List 1.

1. The following data for the slab are loaded: f_c , ϕ_x , ϕ_y , h , h_c , L_x , L_y and E_s .
2. A loop is started where the axial force in x-direction is increased in each step.
 - a. A loop is started where the bending moment in x-direction is increased in each step.
 - i. $n=E_s/E_c$ is calculated.
 - ii. D_y and D_{xy} are calculated using n and Figure 7.1
 - iii. The maximum deflection is determined according to formula (7.4.4).
 - iv. The transverse load is determined according to formula (7.4.2).
 - v. If the maximum stress exceeds the maximum admissible stress the solution for this deflection and transverse load is disregarded.
 - b. The maximum deflection versus transverse load is plotted and the maximum transverse load and the corresponding load is determined for a given axial force.
3. The axial load as a function of the maximum transverse load is plotted.

List 1. Description of the calculation procedure.

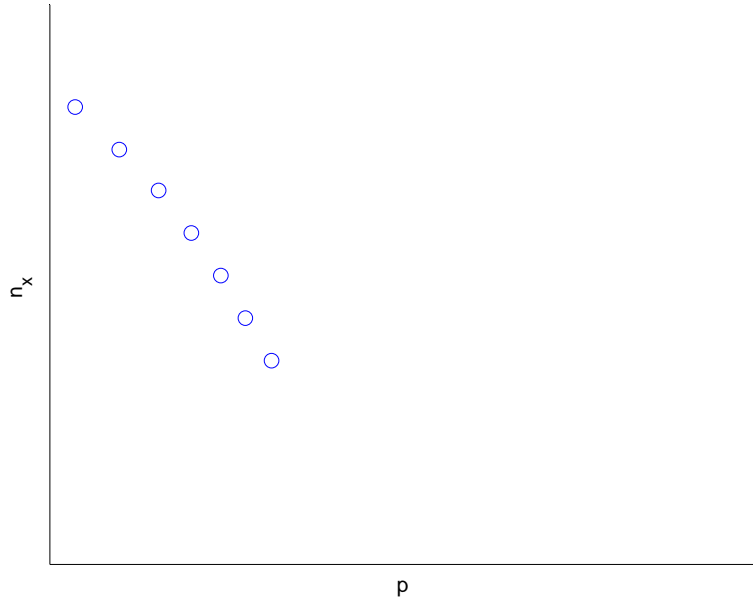


Figure 7.28 Axial force as a function of transverse load.

7.4.1.1 Influence of the loading procedure

Tests made by MacGregor, [6], indicate that the loading procedure influences the load carrying capacity. This can not be explained by the present method. Indeed, we may show that the loading procedure is without influence if the modulus of elasticity is kept constant. In Figure 7.29 the solid line shows how the slab behaves if it is loaded with a transverse load first and then with a lateral load. The dotted line shown the opposite loading procedure. Both failure by instability and by material failure are covered. It is seen that both loading procedures lead to the same result.

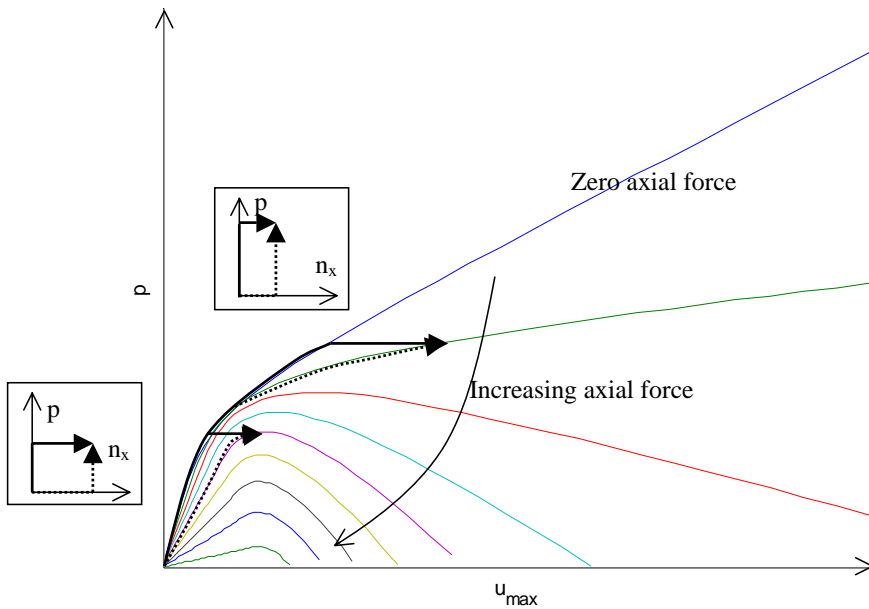


Figure 7.29 Transverse load as a function of maximum deflection for different axial loads.

Such are the facts when the modulus of elasticity remains constant. However, it is well known that this is actually not true for concrete because of its nonlinear behaviour. To take this into account we may assume that the modulus of elasticity is a function of the maximum stress, meaning that a higher stress leads to a lower modulus of elasticity. As an example we might assume a modulus of elasticity of the form:

$$E_c = 1000 f_c \left(1 - \frac{1}{2} \frac{\sigma_{c, \max}}{f_c} \right) \quad (7.4.5)$$

Here $\sigma_{c,max}$ is the maximum compressive stress and f_c is the compressive strength of the concrete. An assumption of this kind may lead to quite different behaviour of the slab as illustrated in Figure 7.30.

The red lines illustrate the behaviour of the slab if it is loaded by a relatively large transverse load. The solid line is valid when the transverse load is applied first and the dotted line is valid if the axial load is applied first. It is seen that in this case the two loading procedures do not lead to the same axial load even though the transverse load is the same.

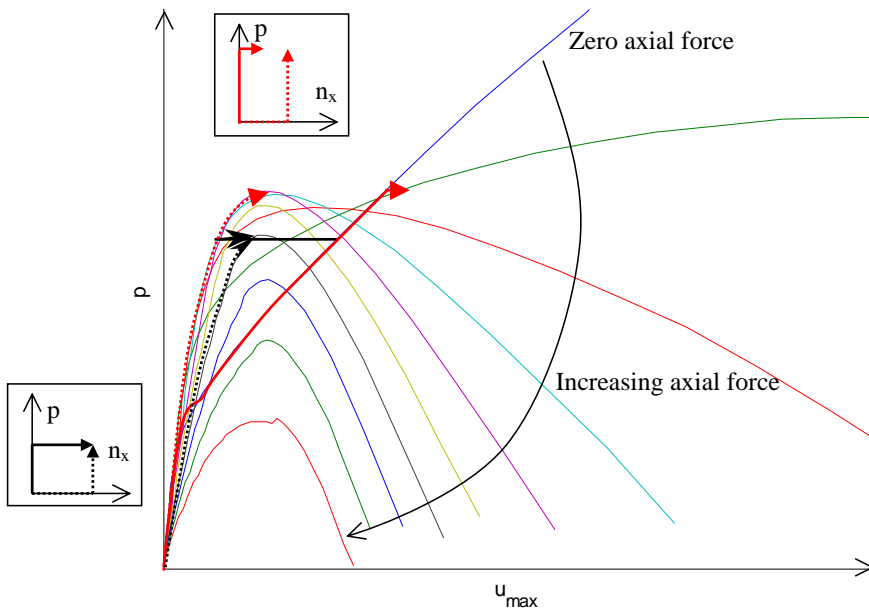


Figure 7.30 Transverse load as a function of maximum deflection for different axial loads.

The black lines illustrate the behaviour if the transverse load is relatively low. In this case both procedures result in the same transverse and axial load. Nevertheless, attention should be given to the fact that if the transverse load is applied first the maximum deflection will decrease and then increase again. Such behaviour will of course influence the behaviour of the concrete since some of the concrete that was cracked starts to be compressed. This fact is not taken into consideration in this investigation.

The results are illustrated by some data from tests, [11].

Figure 7.31 and Figure 7.32 show how two different levels of axial load for the same level of transverse load may be reached.

Figure 7.33 illustrates how the deflection of the slab may decrease as the axial load is increased.

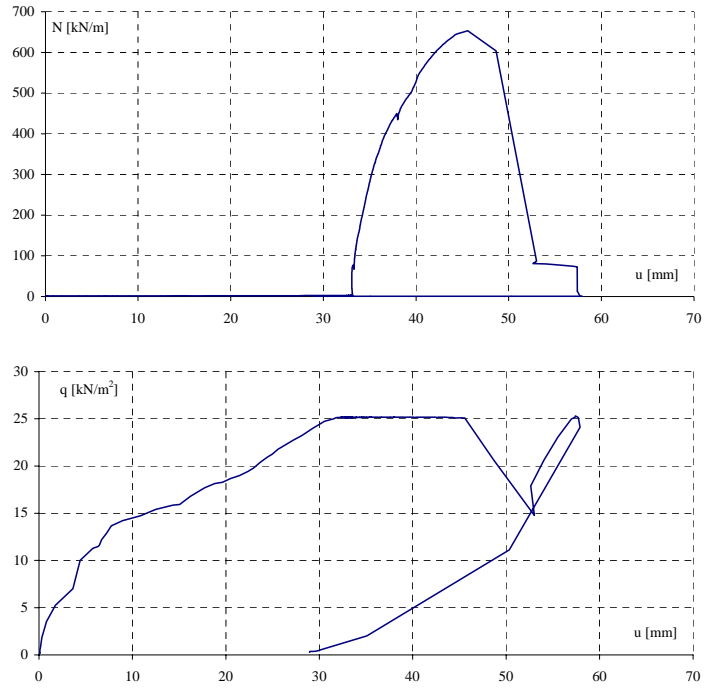


Figure 7.31. The loading curves for slab no 6 in [11].

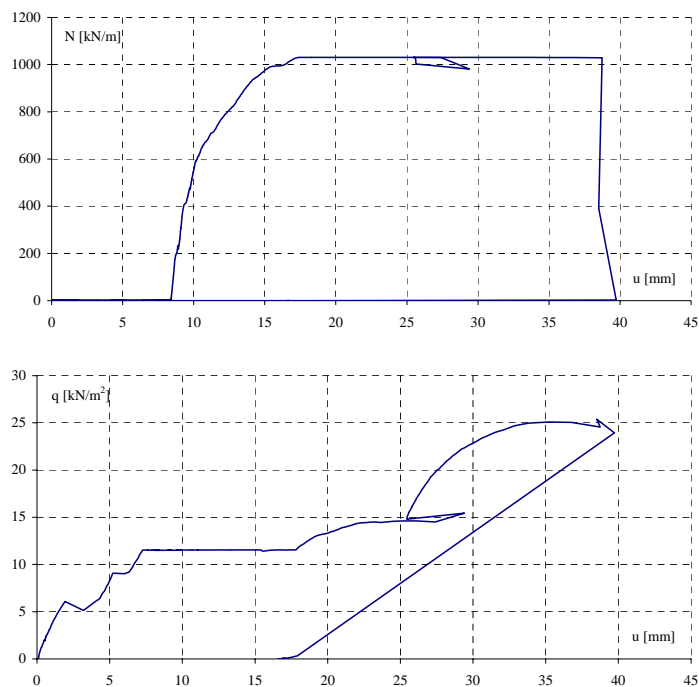


Figure 7.32. The loading curves for slab no 16 in [11].

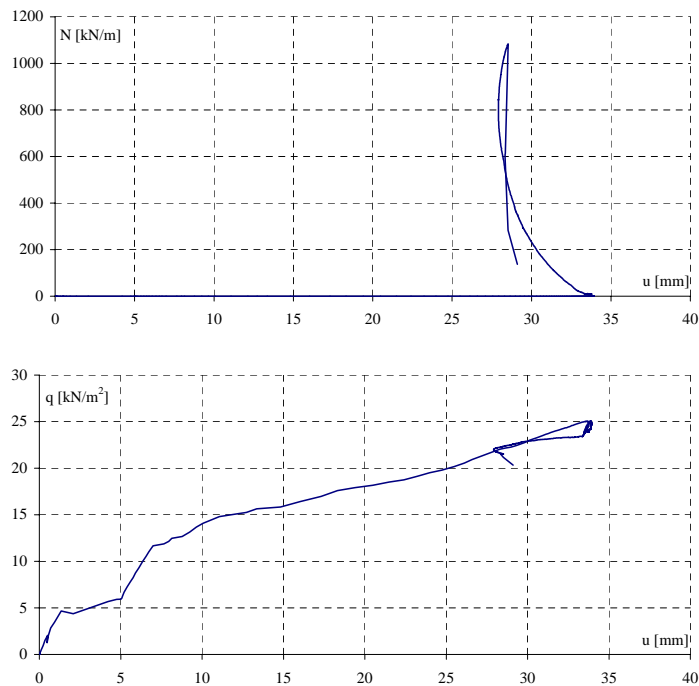


Figure 7.33 The loading curves for slab no 4 in [11]

8 Theory compared with tests

In this section we demonstrate how the methods described in the previous sections may be used to calculate the load carrying capacity for an actual slab that has been tested. The test series was carried out by Larz Z. Hansen and the author, see[11].

In this investigation a square slab loaded with axial force in the x-direction was examined for different combinations of axial force and transverse load.

The main data and results are given in Table 8.1 and Table 8.2.

| No | f_c | E_c | f_Y | h | Layer | A_{sx} | h_{cx} | ρ_{0x} | l_x | h_{cy} | A_{sy} | ρ_{0y} | l_y |
|----|-------|-------|-------|-------|-------|----------------------|----------|-------------|-------|----------|----------------------|-------------|-------|
| | [MPa] | [MPa] | [MPa] | [mm] | | [mm ² /m] | [mm] | [] | [mm] | [mm] | [mm ² /m] | [] | [mm] |
| 1 | 62,5 | 14495 | 593 | 63,42 | 1 | 523,599 | 35 | 0,0083 | 2000 | 25 | 523,599 | 0,00826 | 2000 |
| 2 | 56,0 | 17545 | 593 | 61,38 | 1 | 523,599 | 35 | 0,0085 | 2000 | 25 | 523,599 | 0,00853 | 2000 |
| 3 | 60,4 | 18081 | 593 | 61,66 | 1 | 523,599 | 35 | 0,0085 | 2000 | 25 | 523,599 | 0,00849 | 2000 |
| 4 | 59,5 | 17425 | 593 | 62,03 | 1 | 523,599 | 35 | 0,0084 | 2000 | 25 | 523,599 | 0,00844 | 2000 |
| 5 | 58,8 | 17662 | 593 | 61,63 | 1 | 523,599 | 35 | 0,0085 | 2000 | 25 | 523,599 | 0,0085 | 2000 |
| 6 | 64,6 | 18688 | 593 | 61,37 | 1 | 523,599 | 35 | 0,0085 | 2000 | 25 | 523,599 | 0,00853 | 2000 |
| 7 | 64,0 | 18466 | 593 | 61,26 | 1 | 523,599 | 35 | 0,0085 | 2000 | 25 | 523,599 | 0,00855 | 2000 |
| 8 | 61,4 | 17718 | 593 | 60,99 | 1 | 523,599 | 35 | 0,0086 | 2000 | 25 | 523,599 | 0,00858 | 2000 |
| 9 | 66,7 | 18744 | 593 | 61,56 | 1 | 523,599 | 35 | 0,0085 | 2000 | 25 | 523,599 | 0,00851 | 2000 |
| 16 | 66,7 | 19394 | 593 | 61,48 | 1 | 523,599 | 35 | 0,0085 | 2000 | 25 | 523,599 | 0,00852 | 2000 |

Table 8.1. The data for the reinforced concrete slabs, see [11] for further details. It should be noted that h_c in this case is the distance from the top of the slab to the reinforcement

| No | q | N_x | u | Notes |
|----|----------------------|--------|------|----------------------|
| | [kN/m ²] | [kN/m] | [mm] | |
| 1 | 5,3 | 0,0 | 1,6 | Test slab no failure |
| 2 | 49,8 | 0,0 | 62 | Test slab no failure |
| 3 | 74,5 | 0,0 | 78 | Material failure |
| 4 | 21,5 | 1084,1 | 29 | Rig failure |
| 5 | 33,2 | 462,9 | 53 | Stability failure |
| 6 | 25,1 | 653,3 | 46 | Stability failure |
| 7 | 41,5 | 436,0 | 61 | Stability failure |
| 8 | 16,7 | 800,0 | 42 | Stability failure |
| 9 | 8,5 | 1103,4 | 17 | Material failure |
| 16 | 25,1 | 1030,1 | 37 | Material failure |

Table 8.2. Results from tests.

The calculations in this section will be based on the following data for the slab:

$f_c=62\text{MPa}$, $L_x=L_y=2000\text{mm}$, $h=62\text{mm}$, $h_c=31\text{mm}$, $\phi_x=\phi_y=0.0085$ (one layer of reinforcement). It should be noted that in this case h_c is the distance from the top of the slab to the reinforcement. Also it should be noted that in Table 8.2 the comment “material failure” means material failure at the place where the axial force was applied, i.e. a local failure.

The moduli of elasticity are:

$$\begin{aligned}
 E_s &= 2 \cdot 10^5 \text{ MPa} \\
 E_{0c} &= \min \left\{ \begin{array}{l} 1000 f_c \\ \frac{3}{4} 51000 \frac{f_c}{f_c + 13} \end{array} \right. \\
 k &= 0.8 - 400 \frac{f_c}{E_{0c}} \quad f_c \text{ in MPa} \\
 E_c &= \left(1 - k \frac{\sigma_{\max}}{f_c} - (1 - k) \frac{\sigma_{\min}}{f_c} \right)
 \end{aligned} \tag{7.4.6}$$

where σ_{\max} and σ_{\min} is the maximum and minimum compressive strength in the section, respectively.

Furthermore it is assumed that material failure will take place when the maximum stress in the concrete exceeds $1.25f_c$.

These assumptions are basically those given in the Danish Code of Practice DS411 and represent a simple way of taking the nonlinear behaviour of the concrete into account. Maximum and minimum stresses should strictly speaking be taken as the maximum and minimum principal stresses. However, determination of the principal stresses is not possible on the basis of the present constitutive equations. The reason is that we have assumed that the stiffnesses are independent of each other, which means that the depth of the compression zone when dealing with the torsional stiffness may not be the same as the depth of the compression zone when dealing with the bending stiffnesses. Thus it is not possible to make any correct calculation of the principal stresses. Instead it is assumed that the actions in the x -direction are the dominating ones so that the x -direction may be considered one of the principal directions. Hence the maximum and minimum stresses in formula (7.4.6) are the maximum and minimum stresses in the x -direction.

A description of the computer program may be found in Appendix 11.1. Results of the calculations may be seen in Figure 8.1 to Figure 8.3

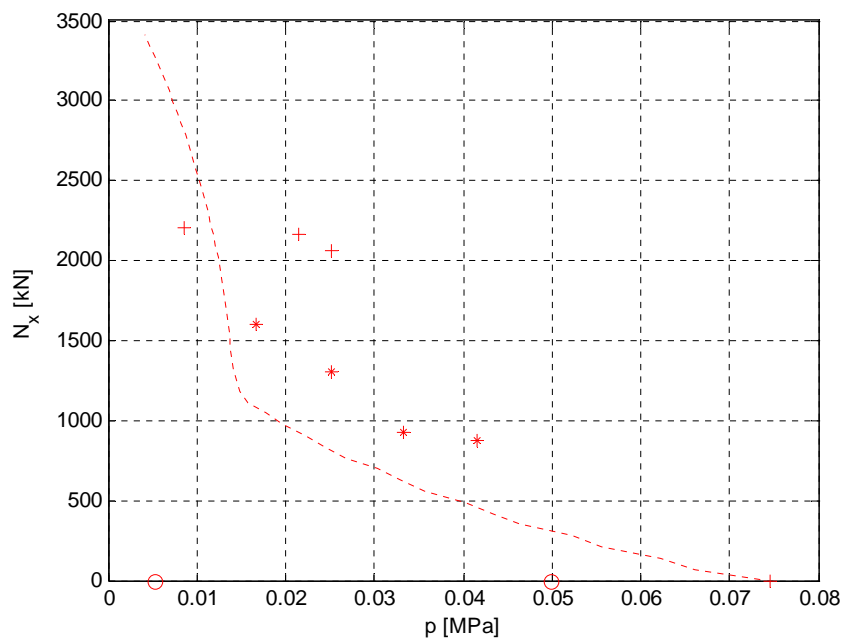


Figure 8.1 Axial force as a function of lateral load. * marks failure by instability, + marks rig failure or material failure and o marks slabs that have not been loaded to failure.

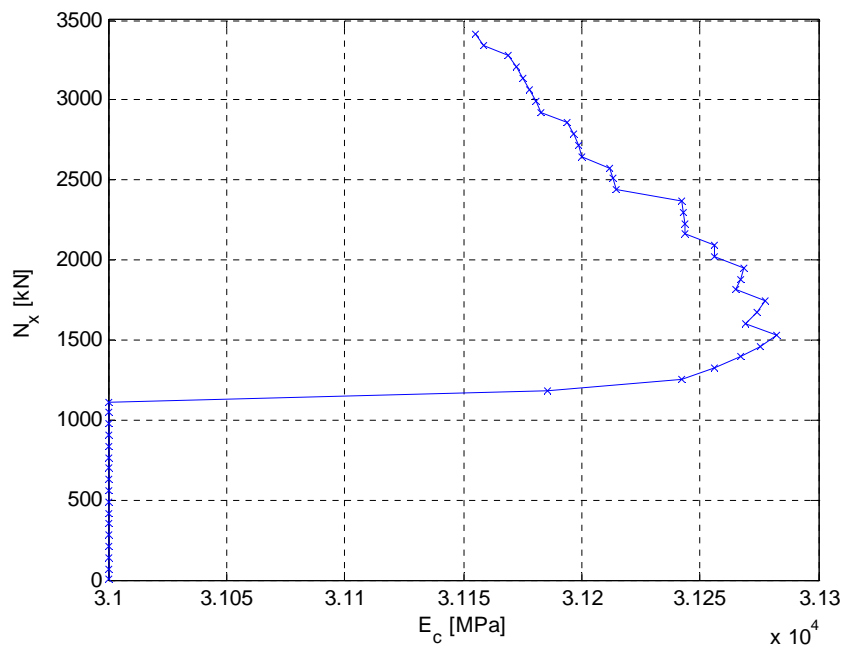


Figure 8.2 Axial force as a function of modulus of elasticity.

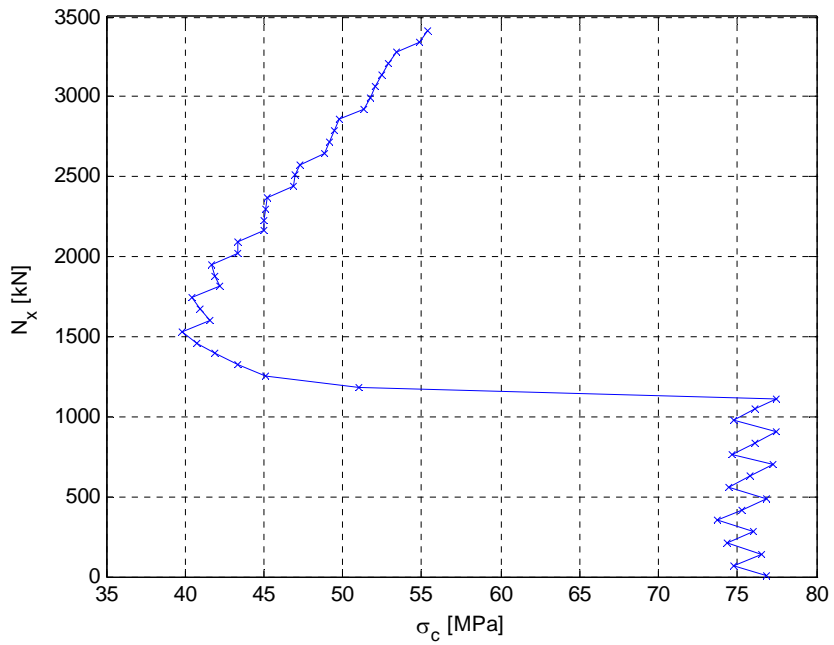


Figure 8.3 Axial force as a function of maximum stresses.

It appears that the calculated values generally are lower than the test results. Only three test values are lower than the calculated ones. Two of these values are valid for a slab that was not tested to failure and in the third test there was material failure. This means that the stability load might have been higher.

The agreement is fairly good considering the simplicity and the assumptions made. The method underestimates the load carrying capacity somewhat. The main reason is the disregarding of the variation of the bending stiffness in the x -direction.

Before we illustrate how the result may be improved we evaluate the variation of the modulus of elasticity. Figure 8.2 shows that the modulus of elasticity varies less than 2%. Therefore it is natural to investigate the effect of using only one modulus of elasticity instead of a varying modulus of elasticity. We thus decide to use the modulus of elasticity found by formula (7.4.6) by assuming that the cross-section is cracked ($\sigma_{min}=0$) and the maximum stress is $1.25f_c$. In this case we get the modulus of elasticity 31000MPa ($=500f_c$). The influence of this assumption may be seen in Figure 8.4.

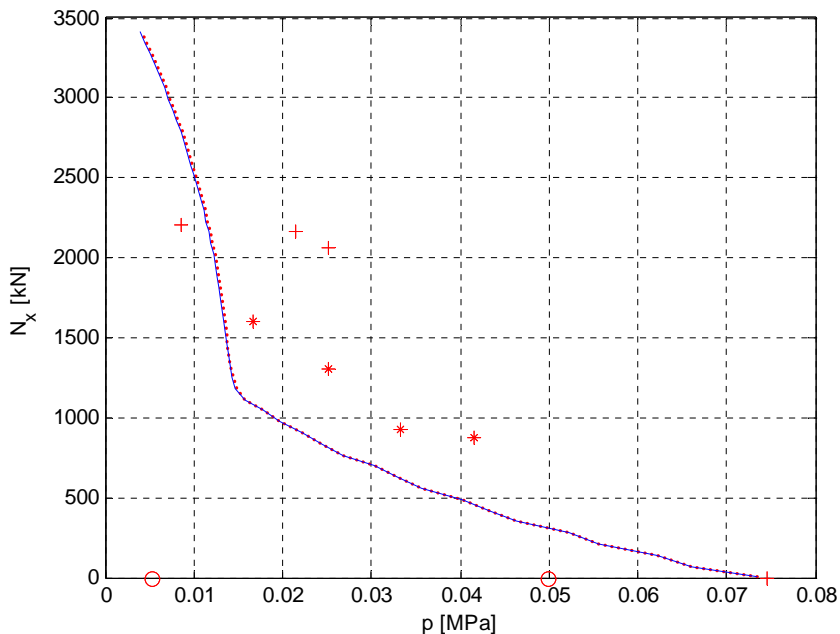


Figure 8.4 Axial force as a function of lateral load. Blue solid line is based on constant bending stiffness, constant torsional stiffness, $h_c/h=1/2$ and constant modulus of elasticity. Red dotted line is based on the same assumptions expect for the modulus of elasticity which is varied according to formula (7.4.6).

As seen in Figure 8.4, the influence is insignificant. Therefore, we shall assume that the modulus of elasticity is constant in what follows.

Another assumption that could be discussed, is the assumption that the reinforcement is placed in the centre. It was in fact placed $\pm 5\text{mm}$ from the centre. In the x -direction the reinforcement was placed 5mm closer to the bottom of the slab, thus the stiffness is underestimated. The opposite is valid for the y -direction. If we take these facts into consideration formula (7.4.11) in Appendix 11.1 should be replaced with the following formulas:

$$\begin{aligned} \frac{D_y}{E_c h^3} &= -6.9793 \cdot 10^{-8} n^4 + 3.6694 \cdot 10^{-6} n^3 - 7.8220 \cdot 10^{-5} n^2 + 1.2172 \cdot 10^{-3} n \\ \frac{D_{xy}}{E_c h^3} &= -1.0145 \cdot 10^{-7} n^4 + 5.1966 \cdot 10^{-6} n^3 - 1.0919 \cdot 10^{-4} n^2 + 1.6956 \cdot 10^{-3} n \end{aligned} \quad (7.4.7)$$

The result of these changes are shown in Figure 8.5. It appears that the changes do not significantly change the results. So we go back to the assumption that the reinforcement is placed in the centre.

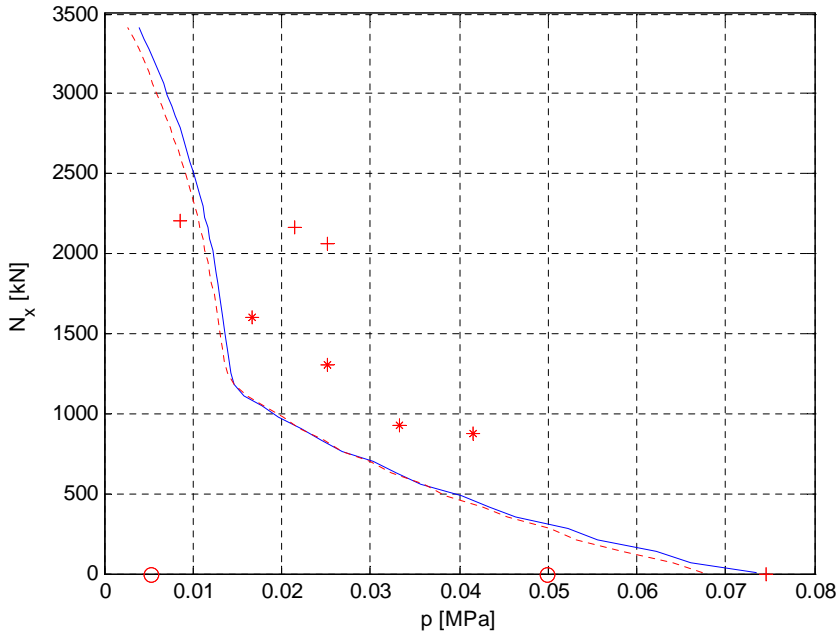


Figure 8.5 Axial force as a function of lateral load. Blue solid line is based on constant bending stiffness, constant torsional stiffness, $h_c/h=1/2$ and constant modulus of elasticity. Red dotted line is based on the same assumptions expect for the position of the reinforcement that were $h_{cx}=36\text{mm}$ and $h_{cx}=26\text{mm}$. Note that these measurements are from the top of the slab to the centre of the reinforcement.

Next we turn our attention to the assumption of using a lower value of the bending stiffness in the x -direction throughout the slab. To check this assumption the calculations are carried out using numerical integration with varying bending stiffness.

Formula (7.4.2) becomes:

$$p = \frac{1}{16} u_{\max} \pi^4 \frac{K_{\text{var}} \frac{8L_y^3 L_x^3}{u_{\max}^2 \pi^2} + \pi^2 L_x^4 D_y + 2\pi^2 D_{xy} L_x^2 L_y^2 - L_y^4 L_x^2 n_x}{L_x^2 L_y^4} \quad (7.4.8)$$

where K_{var} is calculated numerically as:

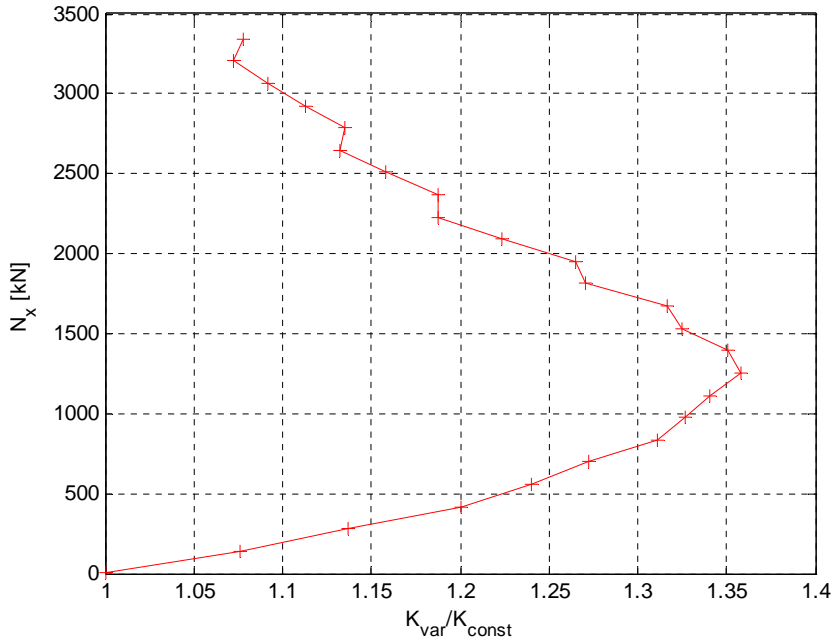
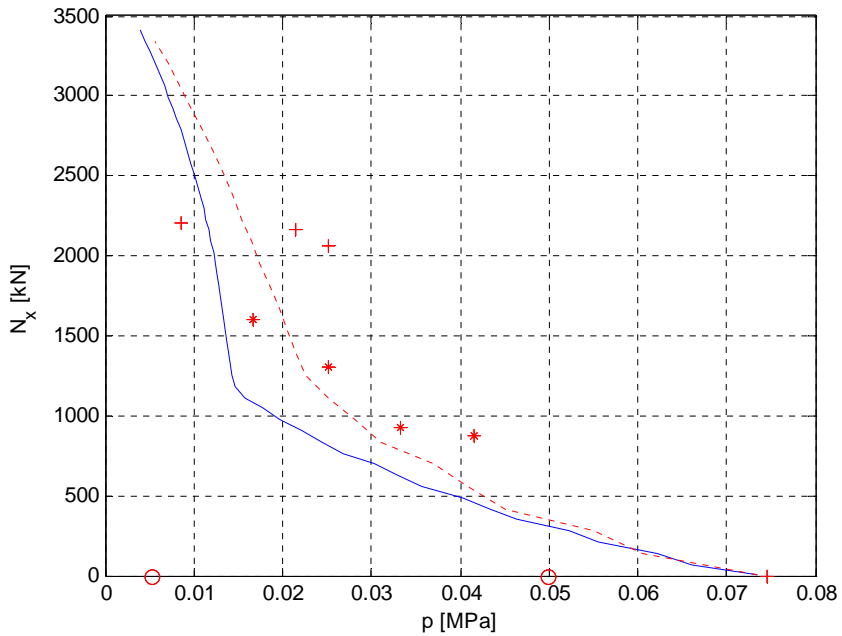
$$K_{\text{var}} = \frac{1}{2} \int \int D_x \kappa_x^2 dx dy \quad (7.4.9)$$

For comparison, if the variation of the bending stiffness is not taken into account, the K value, indexed const, is:

$$K_{\text{const}} = \frac{1}{8} \frac{L_y u_{\max}^2 \pi^4 D_x}{L_x^3} \quad (7.4.10)$$

As required, inserting (7.4.10) into (7.4.8) leads to (7.4.2).

The ratio K_{var} over K_{const} varies as shown in Figure 8.6. The slab has been subdivided into 5 times 5 elements and the correct bending stiffness in the x -direction is determined iteratively until an accuracy of 1% is achieved. The procedure is similar to the procedure for determining the modulus of elasticity described in section 11.1.


 Figure 8.6 Axial force as a function of K_{var}/K_{const}

 Figure 8.7 Axial force as a function of lateral load. Blue solid line is based on constant bending stiffness, constant torsional stiffness, $h_c/h=1/2$ and constant modulus of elasticity. Red dotted line is based on the same assumptions expect for the bending stiffness which varies throughout the slab.

It is seen from Figure 8.6 that the deviation of K is more than 35% in some cases. Figure 8.7 illustrates the changes obtained in the load carrying capacity diagram.

It appears that the difference between the two calculations is significant and it most pronounced for axial forces about 1000-1500kN.

The agreement between the more accurate calculations and the test results is good.

9 Conclusion

In this paper it is shown that the use of an upper bound approach for the determination of slab behaviour results in relatively simple calculations. The solutions are believed to be sufficiently correct for many practical purposes and, more important, they demonstrate how to calculate slabs with different torsional- and bending stiffness.

For slabs subjected to transverse load only it is shown that the difference between the torsional- and bending stiffnesses, due to different position of the reinforcement, leads to a difference in the overall slab behaviour of up to a factor of 1.9. This result is valid for a square slab supported at two adjacent sides.

Similar conclusions are reached for slabs subjected to axial force only.

The approach for slabs subjected to both axial force and transverse load is described in general and one test series has been used to verify the method. Good agreement was found.

10 Literature

The list is ordered by year.

- [1] Nielsen, N. J.: Beregninger af Spændinger I Plader, Doktorafhandling ved Den Polytekniske Læreanstalt, København, 1920.
- [2] JOHANSEN, K.W., Brudlinieteorier (Yield line theories), *Copenhagen, Gjellerup, 1943.*
- [3] NIELSEN, M. P. and RATHKJEN, A.: Mekanik 5.1. Del 1 Skiver og plader, *Danmarks Ingeniørakademi, Bygningsafdelingen, Aalborg, Den Private Ingeniørfond, 1981.*
- [4] NIELSEN, M. P. and RATHKJEN, A.: Mekanik 5.1. Del 2 Skiver og plader, *Danmarks Ingeniørakademi, Bygningsafdelingen, Aalborg, Den Private Ingeniørfond, 1981.*
- [5] AGHAYERE, A. O. and MACGREGOR, J. G., Test of reinforced Concrete Plates under Combined In-Plane and Transverse Loads, *ACI Structural Journal*, V. 87, No. 6, pp. 615-622, 1990
- [6] AGHAYERE, A. O. and MACGREGOR, J. G., Analysis of Concrete Plates under Combined In-Plane and Transverse Loads, *ACI Structural Journal*, V. 87, pp. 539-547, September-October 1990.
- [7] MASHHOUR, G. G. and MACGREGOR, J. G., Prediction of the Ultimate Strength of Reinforced Concrete Plates Under Combined Inplane and Lateral Loads, *ACI Structural Journal*, pp. 688-696, November-December 1994.
- [8] MOSEKILDE, E: Topics in nonlinear dynamics, *World Scientific, ISBN 981-02-2764-7, 1996.*
- [9] NIELSEN, M. P.: Limit Analysis and Concrete Plasticity, *Second Edition, CRC Press, 1998.*
- [10] NIELSEN, M. P., HANSEN, L. P. and RATHKJEN, A.: Mekanik 2.2. Del 1 Rumlige spændings- og deformationstilstande, *Institut for bærende konstruktioner og materialer, Danmarks Tekniske Universitet, Aalborg/København 2001.*

- [11] HANSEN, L. Z., GUDMAND-HØYER, T.: Instability of Concrete Slabs,
Department of Structural Engineering and Materials, Master thesis, Technical University of Denmark, 2001
- [12] NIELSEN, M. P.: Beton 2 del 4- Skiver og høje bjælker, *1 udgave, Lyngby, 2002.*
- [13] J. G. SANJAYAN and D. MANICKARAJAH: Buckling analysis of reinforced concrete walls in two-way action, *Bygningsstatiske Meddelelser, Årgang LXXXIV, nr 1, pp.1-20, Marts 2003.*
- [14] T. GUDMAND-HØYER: Stiffness of Concrete Slabs, *R-092, ISSN 1601-2917, ISBN 87-7877-156-0, Technical University of Denmark, 2004*
- [15] S. P. TIMOSHENKO and J. M. GERE: Theory of Elastic Stability, *second edition, ISBN 0-07-085821-7, 1961.*

11 Appendix

11.1 Description of computer program

This is a description of the program used to calculate the load carrying capacity of the slab used in the test series [11].

4. The following data for the slab are loaded: f_c , ϕ_x , ϕ_y , h , h_c , L_x , L_y and E_s .
5. A loop is started where the axial force in x-direction is increased in each step.
 - a. A loop is started where the bending moment in x-direction is increased in each step.
 - i. The modulus of elasticity is assumed to be $E_c = 500f_c$.
 - ii. $n = E_s/E_c$ is calculated.
 - iii. D_y and D_{xy} are calculated for the n -value according to ii. Generally the stiffness may be found from Figure 7.1 (using $n\phi$), but in this case the following formula is used (a polynomial fit to calculated values):

$$\frac{D_y}{E_c h^3} = \frac{D_{xy}}{E_c h^3} = -1.0145 \cdot 10^{-7} n^4 + 5.1966 \cdot 10^{-6} n^3 - 1.0919 \cdot 10^{-4} n^2 + 1.6956 \cdot 10^{-3} n \quad (7.4.11)$$

- iv. A loop is started and runs as long as the difference between the modulus of elasticity and a new modulus of elasticity calculated in the loop is more than 1%. If the difference is large the modulus of elasticity is set to the average of the two.
 1. From the axial force and the bending moment in the x-direction the stiffness and the maximum and minimum stresses are found. The stiffness may be read off Figure 7.1 using $n\phi$ and the stresses found from a simple cross section analysis. In this case the formulas for the stiffness and stresses from [14] are used.

2. The new modulus of elasticity is calculated according to formula (7.4.6).
 3. D_y and D_{xy} are calculated from n using formula (7.4.11).
 - v. The maximum deflection is determined according to formula (7.4.4).
 - vi. The transverse load is determined according to formula (7.4.2).
 - vii. If the maximum stress exceeds $1.25f_c$ the solution for this deflection and transverse load is disregarded.
 - b. The maximum deflection versus transverse load is plotted and the maximum transverse load and the corresponding load is determined for a given axial force.
6. The axial load as a function of the maximum transverse load is plotted.
 7. The test values are plotted.



Report
BYG – DTU R-094
2003
ISSN 1601-2917
ISBN 87-7877-159-5